Quasi-Orthogonal Space-Time Block-Coded OFDM Wireless Mobile Communication Systems using Array-Processing Approach

Thesis submitted in partial fulfillment of the requirement for the award of the degree of

MASTER OF ENGINEERING

In

ELECTRONICS & COMMUNICATION ENGINEERING

Submitted by

Sunil Kumar

Roll no. 801161029

Under the Guidance of

Dr. Amit Kumar Kohli

Assistant Professor, ECED, TU

Electronics and Communication Engineering Department

Thapar University, Patiala-147004 (PUNJAB)

June, 2013

CERTIFICATE

I, **Sunil Kumar** hereby certify that the work, which is being presented in this thesis entitled "**Quasi-Orthogonal Space-Time Block-Coded OFDM Wireless Mobile Communication Systems using Array-Processing Approach**" by me in partial fulfillment of the requirements for the award of degree of Master of Engineering in Electronics and Communication Engineering at Thapar University, Patiala, is an authentic record of my own work carried out under the guidance of **Dr. Amit Kumar Kohli,** Assistant Professor, **Electronics and Communication Engineering Department**, Thapar University, Patiala. The matter presented in this thesis has not been submitted in any other university or institute for the award of the degree of Master of Engineering.

Sunil Kumar

Date 28/06/2013

This is certified that the above statement made by the candidate is correct to the best of my knowledge.

Dr. Amit Kumar Kohli
Assistant Professor, ECED
Thapar University, Patiala
Date 28/06/2013

Countersigned by :

Dr. R. Khanna
Professor & Head, ECED
Thapar University, Patiala
Date 2/7/13

Dr. S. K. Mohapatra
Dean of Academic Affairs
Thapar University, Patiala
Date _____

ACKNOWLEDGEMENT

No volume of words is enough to express my gratitude towards my guide, **Dr. Amit Kumar Kohli**, Assistant Professor, Electronics and Communication Engineering Department, Thapar University, who has been very concerned and has aided for all the material essential for the preparation of this thesis report. He has helped me to explore this vast topic in an organized manner and provided me with all the ideas on how to work towards a research-oriented venture.

I am also thankful to **Dr. Rajesh Khanna**, Head of Department, ECED, **Dr. Kulbir Singh**, P.G. Coordinator and **Dr. Sanjay Sharma,** Professor, ECED for the motivation and inspiration that triggered me for the thesis work.

I would also like to thank the staff members and my colleagues who were always there in the need of the hour and provided with all the help and facilities, which I required, for the completion of my thesis.

Most importantly, I would like to thank my parents and the Almighty for showing me the right direction out of the blue, to help me stay calm in the oddest of the times and keep moving even at times when there was no hope.

Sunil

Sunil Kumar

Roll No. - **801161029**

ABSTRACT

The phenomenon of multipath fading constitutes a fundamental problem in the wireless communication. Researchers have proposed many methods to improve the reliability of communication over wireless communication channels in the presence of fading. MIMO is one of the important techniques used to achieve the diversity gain or multiplexing gain. There are various diversity techniques, in which transmit diversity has the advantage of power and bandwidth efficiency. OFDM is another technique used to combat the effect of frequency-selectivity of multipath fading channel. OFDM also removes the ISI (intersymbol interference). OFDM converts frequency-selective channel into frequency flat fading channel and hence single tape equalizer is required at the receiver end. MIMO-OFDM is an important technique to improve SER performance in the high data transmission rate communication systems.

In this thesis report, QO-STBC designs are used to achieve diversity and coding gain. Orthogonal designs are the optimum choice, which provides full diversity gain and can be decoded by linear processing unit. But unfortunately, orthogonal design with full diversity gain & full code rate does not exist for more than two transmitting antennas for the complex signal constellation. To increase data rate, the quasi- orthogonal design is used, but we have to sacrifice the diversity gain. Computational complexity in QO-STBC design increases and results in more transmission delay. To reduce computational complexity, the array-processing technique is used, in which the received data is converted into parallel streams. Each parallel data stream is decoded simultaneously by the separate OSTBC decoder.

We assume perfect CSI (channel state information) estimation and perfect synchronization. Hence, the effect of channel estimation does not affect the SER performance. Simulation results are investigated for Rayleigh and Nakagami-m fading channels. Multipath fading channel is considered to be time-variant frequency-selective and it is assumed that the channel gain remains constant over K consecutive OFDM symbols (number of symbols used in STBC code design).

Keywords :- *Quasi-orthogonal, space-time block-coding, null space, symbol error rate, array-processing, Hermitian transposition, frequency selective fading.*

TABLE OF CONTENTS

CHAPTER 4 : INTRODUCTION TO FADING IN WIRELESS SYSTEM

CHAPTER 5 : INTRODUCTION TO SPACE-TIME BLOCK-CODED WIRELESS SYSTEM

CHAPTER 6 : MATHEMATICAL ANALYSIS OF BER IN MIMO-OFDM SYSTEM

LIST OF ACRONYMS

3G	third generation
AWGN	additive white Gaussian noise
BER	bit error rate
BPSK	binary phase shift keying
BTS	base trans-receiver station
CDF	cumulative distribution function
CDMA	code division multiplexing access
CP	cyclic prefix
CSI	channel state information
DAB	digital audio broadcasting
DFT	discrete fourier transform
DSL	digital subscriber line
DVB	digital video broadcasting
GI	guard interval
ICI	inter carrier interference
IDF	inverse discrete fourier transform
ISI	inter-symbol interference
LAN	local area network
LOS	line of sight
MAN	metropolitan area network
MCM	multi-carrier modulation
MIMO	multiple-input multiple-output
ML	maximum likelihood decoding
MRRC	maximum ratio receiver combining
STC	space-time code
STBC	space-time block code
STTC	space-time trellis code
OSTBC	orthogonal space-time block code

OFDM	orthogonal frequency division multiplexing
PAN	personal area network
PAPR	peak to average power ratio
PDF	probability density function
PSK	phase shift keying
QAM	quadrature amplitude modulation
QPSK	quadrature phase shift keying
QO-STBC	quasi-orthogonal space-time block code
SQAM	staggered quadrature amplitude modulation

LIST OF FIGURES

LIST OF TABLES

CHAPTER 1

INTRODUCTION

1.1 Background

Wireless communications is one of the fastest growing segments in the communications industry. It has captured the attention of the media and the imagination of the public. Wireless communication mainly categorized for media (voice and video), and data. Under media, cellular systems have experienced exponential growth over the last decade and there are currently about two billion users worldwide. Indeed, cellular phones have become a critical business tool and part of everyday life in most developed countries. For data applications, wireless local area networks currently replace wired networks in many homes, businesses, and campuses. Many new applications, including wireless sensor networks, automated highways and factories, smart homes and appliances, and remote telemedicine are emerging from research ideas. The explosive growth of wireless systems integrated with computers suggest a bright future for wireless networks systems. However, many technical challenges remain in designing robust wireless networks, that deliver the performance necessary to support emerging applications. The gap among current, emerging systems and the vision for future wireless applications indicates that, much work remains to be done to make this vision a reality.

OFDM concept is very efficient in frequency selective fading due to lesser bandwidth of channel, but this decreases the signal power. So, power of signal should be increased. Transmitting power is not a possible solution in fading channel due to almost unfeasible required power. Another solution is the diversity technique which increase signal to noise ratio. Here STBC [1] is used which provides diversity gain. Diversity gain and data transmission rate are reciprocal to each other in generalized complex orthogonal design [2]. So, there should be tradeoff between diversity gain and data rate.

1.2 Introduction to the Wireless Problem

Due to an explosion of demand for high-speed wireless services, such as wireless internet, email, stock quotes and cellular video conferencing, wireless communication has become one of the most exciting fields in modern engineering. However, development of such products and services poses a serious challenge: how can we support the high data rates and capacity required for these applications with the severely restricted resources offered in a wireless channel? The obstacles associated with wireless environment are difficult to overcome. Interference from other users and inter-symbol interference (ISI) from multiple paths of one's own signal are serious forms of distortion. Furthermore, when transmit and receive antennas are in relative motion, the Doppler effect will spread the frequency spectrum of received signals. This results in time varying channel characteristics. Many systems must function without a line-of-sight (LOS) path between transmit and receive antennas, thus pure Rayleigh fading may completely attenuate a signal. Additionally, the usual additive white Gaussian noise (AWGN) can corrupt the signal.

Besides the above difficulties, there are extremely limited bandwidth and stringent power limitations on both the mobile unit (for battery conservation) and the base station (to satisfy government safety regulations). To conserve the bandwidth resources, we maximize spectral efficiency by packing as much information as possible into a given bandwidth. A solution to the bandwidth and power problem is the cellular concept, in which frequency bands are allocated to small, low power cells and reused at the cells far away. However, this idea alone is not enough. We must look to other means, such as space-time coding to increase data rate, capacity and spectral efficiency.

1.3 Motivation

Multi-carrier modulation (MCM) has recently gained fair degree of prominence among modulation schemes due to its intrinsic robustness in frequency selective fading channels. This is one of the main reason to select MCM a candidate for systems such as Digital Audio and Video Broadcasting (DAB and DVB), Digital Subscriber Lines (DSL), and Wireless local area networks (WLAN), metropolitan area networks (MAN), personal

area networks (PAN), home networking and even beyond 3G wide area networks (WAN). Orthogonal Frequency Division Multiplexing (OFDM), a multi-carrier transmission technique that is adopted in different communication applications. OFDM systems support high data rate transmission.

However, OFDM systems have the undesirable feature of a large peak to average power ratio (PAPR) of the transmitted signals. The transmitted signal has a non-constant envelope and exhibits peaks whose power strongly exceeds the mean power. Consequently, to prevent distortion of the OFDM signal, the transmit amplifier must operate in its linear regions. Therefore, power amplifiers with a large dynamic range are required for OFDM systems. Reducing the PAPR is pivotal to reducing the cost of OFDM systems. Wireless systems always give several errors to the transmitted bits due to several transmission and system impediments. The techniques of power control also increase the bit error rate in end to end transmission. To address this need, communication engineers have combined technologies suitable for high rate transmission with error correction codes. Forward error correction (FEC) is one of the popular techniques. FEC or similar coding techniques allow the system to operate with lower power, allow the system to give more range even under other uncontrolled impediments of the system.

1.4 Technological Review

It is well known that Chang proposed the original OFDM principles in 1966 and successfully achieved a patent in Jan, 1970. Later on, Saltzberg analyzed the OFDM performance and observed that the crosstalk was the severe problem in this system. Although each subcarrier in the principal OFDM system overlapped with the neighborhood subcarriers, the orthogonality can still be preserved through the staggered QAM (SQAM) technique. However, the difficulty will emerge when a large number of subcarriers are required. In some of the early OFDM applications, the number of subcarriers can be chosen up to 34, allowing 34 symbols with redundancy of guard time interval to eliminate inter-symbol interference (ISI). However, it should be required more subcarriers. The synchronization and coherent demodulation would induce a very complicated OFDM scheme requiring additional hardware cost.

In 1971, Weinstein and Ebert proposed a modified OFDM system in which the Discrete Fourier Transform (DFT) was applied to generate the orthogonal subcarriers waveforms. Their scheme reduced the implementation complexity significantly by making use of the inverse DFT (IDFT) modules and the digital-to-analog converters. In their proposed model, baseband signals were modulated by the IDFT in the transmitter and then demodulated by DFT in the receiver. Therefore, all the subcarriers were overlapped with others in the frequency domain, while the DFT modulation still assures their orthogonality. Cyclic prefix (CP) or cyclic extension was first introduced by Peled and Ruiz in 1980 for OFDM systems. In their scheme, conventional null guard interval is substituted by cyclic extension for fully loaded OFDM modulation. As a result, the orthogonality among the subcarriers was guaranteed. With the trade-off of the transmitting energy efficiency, this new scheme can result in a phenomenal ICI (Inter Carrier Interference) reduction. Hence, it has been adopted by the current IEEE standards.

In 1980, Hirosaki introduced an equalization algorithm to suppress both inter symbol interference (ISI) and ICI, which may have resulted from a channel distortion, synchronization error or phase error. In the meantime, Hirosaki also applied QAM modulation, pilot tone and trellis coding techniques in his high-speed OFDM system, which operated in voice-band spectrum. In 1985, Cimini introduced a pilot-based method to reduce the interference originating from the multipath and co-channels. In 1989, Kalet suggested a subcarrier-selective allocating scheme. He allocated more data through transmission of "good" subcarriers near the center of the transmission frequency band, these subcarriers will suffer less channel distortion.

In the 1990s, OFDM systems have been exploited for high data rate communications. In the IEEE 802.11 standard, the carrier frequency can go up as high as 2.4 GHz or 5 GHz. Researchers tend to pursue OFDM operating at even much higher frequencies now a days. Coded OFDM allows the exploitation of frequency diversity and it provides a greater immunity to impulse noise and fast fades. One of the major drawbacks of OFDM is its high PAPR. This limits the transmission range and requires that the transmit amplifiers have a large dynamic range in linear region. In many low-cost operations, the disadvantages outweigh all the benefits of OFDM. The idea of jointly solving the PAPR and the error correcting code design problem is first addressed using block codes. Similarly, Davis et al.

obtain a class of low PAPR codes with minimum distance based on cossets of Reed-Muller codes.

1.5 Problem Formulation

Due to the amplification of the noise power when carrying out the array processing, the SER (symbol error rate) performance of the proposed decoder is degraded by roughly 3 dB, which decrease the maximum possible data transmission rate. The SER performance worsens off when the maximum Doppler shift increases, since in the array processing and decoder units, we assume that the four consecutive OFDM symbols suffer from the same fading. When the Doppler shift goes higher, the mismatch for the channel responses in the four consecutive OFDM symbols will become larger. Obviously, assuming the same fading over the four consecutive OFDM symbols may result in a poor SER performance. Channel model we consider is of two kinds of fading, i.e., time selective and frequency selective. Frequency-selective fading can be mitigated by the added GI (Guard Interval). However, to eliminate time-selective fading, additional time domain equalization should be adopted. Space-time block coding is used to provide diversity gain, which is bandwidth and power efficient technique. Another technique, OFDM is used to overcome the frequency selectivity of channel.

1.6 Organisation of thesis

Chapter 1 : Chapter 1 gives the introduction of wireless communication, and the problems associated with the wireless communication systems.

Chapter 2 : In Chapter 2, literature survey about STBC-OFDM technique and computational complexity in decoding is given.

Chapter 3 : Introduction of OFDM and synchronization problems are explained in chapter third.

Chapter 4 : Chapter 4 gives the introduction of attenuation and fading models.

Chapter 5 :Chapter 5 gives details about space-time coding.

Chapter 6 : Mathematical analysis of bit error rate performance is given for MIMO-OFDM.

Chapter 7 : Array-processing technique is used in QO-STBC to reduce computational complexity at the receiver.

Chapter 8 : Simulation results are given in chapter eight.

At last, concluding remarks about the thesis report and future scope is given.

CHAPTER 2

LITERATURE SURVEY

Alamouti [1]

This paper presents a simple two-branch transmit diversity scheme. Using two transmit antennas and one receive antenna, this scheme provides the same diversity order as maximal-ratio receiver combining (MRRC) with one transmit antenna and two receive antennas. It is also shown that the scheme may easily be generalized to two transmit antennas and M receive antennas to provide a diversity order of 2M. The new scheme does not require any bandwidth expansion, any feedback from the receiver to the transmitter and its computation complexity is similar to MRRC.

In this paper, basically two transmit antennas are used, because complex orthogonal space-time coding exist only for n=2. Orthogonality leads to simple linear processing at receiver which makes maximum likelihood decoding simple. The performance of the new scheme with two transmitters and a single receiver is 3 dB worse than two-branch MRRC. The 3 dB penalty is occurred because the simulations assume that each transmit antenna radiates half the energy in order to ensure the same total radiated power as with one transmit antenna. If each transmit antenna in the new scheme was to radiate the same energy as the single transmit antenna for MRRC, the performance would be identical. In other words, if the BER was drawn against the average SNR per transmit antenna, then the performance curves for the new scheme would shift 3 dB to the left and overlap with the MRRC curves. Nevertheless, even with the equal total radiated power assumption, the diversity gain for the new scheme with one receive antenna at a BER of 10 is about 15 dB. Similarly, assuming equal total radiated power, the diversity gain of the new scheme with two receive antennas at a BER of 10 is about 24 dB, which is 3 dB worse than MRRC with one transmit antenna and four receive antennas. However, the 3 dB reduction of power in each transmit chain translates to cheaper, smaller or less linear power amplifiers. A 3 dB reduction in amplifiers power handling is very significant and may be desirable in some cases. It is often less expensive (or more desirable from inter modulation distortion effects) to employ two half-power amplifiers rather than a single full power amplifier. Diversity

improvement is done when different antennas are sufficiently uncorrelated (less than 0.7 correlation) and that they have almost equal average power (less than 3 dB difference). If two receive antennas are used to provide diversity at the base station receiver, they must be on the order of ten wavelengths apart to provide sufficient decorrelation to get the same diversity improvement at the remote units it is sufficient to separate the at the remote station by about three wavelengths. It is due to the difference in the nature of the scattering environment in the proximity of the remote and base stations

V. Tarokh, H. Jafarkhani and A. Calderbnk [2]

Orthogonal designs those used in construction of space–time block codes make maximum likely decoding simple by linear processing at receiver but unfortunately, exist for few sporadic values of n. Subsequently, a generalization of orthogonal designs [2] is shown to provide space–time block codes for both real and complex constellations for any number of transmit antennas. These codes achieve the maximum possible transmission rate for any number of transmit antennas using any arbitrary real constellation such as PAM exist for n=2, 4 and 8. For an arbitrary complex constellation such as PSK and QAM, space–time block codes are designed that achieve 1/2 of the maximum possible transmission rate for any number of transmit antennas. For the specific cases of two, three, and four transmit antennas, space–time block codes are designed that achieve, respectively, all, 3/4 and 1/2 of maximum possible transmission rate using arbitrary complex constellations [2].

Junwoo Jung, Kwon and Park [3]

A superposition-based adaptive modulated STBC (SPAM-STBC) for MIMO-OFDM [3] systems improves adaptive modulation for optimization of space time block coding (STBC). When transmit antennas have the different channel conditions, the fixed adaptive modulated STBC selects the same modulation based on averaging of the multiple channel gains. If the different modulation is selected to each transmit antenna, the STBC decoding problem occurs. In this letter, we select the optimal modulation corresponding to each channel condition by the super positioned space time encoding and decoding, proposed SPAM-STBC scheme outperforms both the fixed and adaptive modulated STBC schemes by the maximum 0.407 bits/sec/Hz in terms of spectral efficiency.

When the channel condition of each transmit antenna is different and uncorrelated, it can increase the effective spectral coding.. If each of transmitting symbols has a different

modulation level according to the channel condition of each antenna, the STBC decoding error occurs due to the unmatched channel condition, e.g. 16-QAM modulated symbols are transmitted over the channel condition of QPSK. The objective of the proposed SPAM-STBC is to increase spectral efficiency by selecting the optimal modulation with the superposition coding, when the channel conditions between different transmitting antennas are different and uncorrelated. In MIMO-OFDM systems, since the correlation is very high among contiguous subcarriers of each antenna and the number of the selected subcarriers is small, e.g. between 2 and 4, we assume that those subcarriers experience the highly correlated channel coefficient.

Hamid Jafarkhani [4]

It has been shown that a complex orthogonal design that provides full diversity and full transmission rate for a space–time block code [2] is not possible for more than two antennas. Previous attempts have been concentrated in generalizing orthogonal designs which provide space–time block codes with full diversity and a high transmission rate. In this work, we design rate one codes which are quasi-orthogonal [4] and provide partial diversity. The decoder of the proposed codes works with pairs of transmitted symbols instead of single symbols.

Chau Yuen and Yong Liang Guan [5]

In this paper, we consider a quasi-orthogonal (QO) space-time block code (STBC) with minimum decoding complexity (MDC-QO-STBC) [5]. We formulate its algebraic structure and propose a systematic method for its construction. We show that a maximum-likelihood (ML) decoder for this MDC-QOSTBC, for any number of transmit antennas, only requires the joint detection of two real symbols. Assuming the use of a square or rectangular quadratic-amplitude modulation (QAM) or multiple phase-shift keying (MPSK) modulation for this MDC-QOSTBC, we also obtain the optimum constellation rotation angle [6], in order to achieve full diversity and optimum coding gain. We show that the maximum achievable code rate of these MDCQO- STBC is 1 for three and four antennas and 3/4 for five to eight antennas [4]. We also show that the proposed MDC-QOSTBC has several desirable properties, such as a more even power distribution among antennas and better scalability in adjusting the number of transmit antennas, compared with the coordinate interleaved orthogonal design (CIOD) and asymmetric CIOD (ACIOD) codes. For the case of an odd

number of transmit antennas, MDC-QO-STBC also has better decoding performance than CIOD.

W. Su and X. G. Xia [6]

Space–time block codes (STBCs) from orthogonal designs proposed by Alamouti [1] and Tarokh–Jafarkhani–Calderbank [2] have attracted considerable attention due to their fast maximum-likelihood (ML) decoding and full diversity. However, the maximum symbol transmission rate of an STBC from complex orthogonal designs for complex signals is only 3/4 for three and four transmit antennas, and it is difficult to construct complex orthogonal designs with rate higher than ½ for more than four transmit antennas. Jafarkhani, Tirkkonen–Boariu–Hottinen, and Papadias–Foschini proposed STBCs from quasi-orthogonal designs, where the orthogonality is relaxed to provide higher symbol transmission rates. With the quasi-orthogonal structure, the quasi-orthogonal STBCs still have a fast ML decoding [7], but do not have the full diversity. The performance of these codes is better than that of the codes from orthogonal designs at low signal-to-noise ratio (SNR), but worse at high SNR. This is due to the fact that the slope of the performance curve depends on the diversity. It is desired to have the quasi-orthogonal STBCs with full diversity to ensure good performance at high SNR. In this paper, we achieve this goal by properly choosing the signal constellations [6]. Specifically, we propose that half of the symbols in a quasi-orthogonal design are chosen from a signal constellation set and the other half of them are chosen from a rotated constellation. The resulting STBCs can guarantee both full diversity and fast ML decoding [2]. The proposed codes outperform the codes from orthogonal designs at both low and high SNRs.

Chang-Kyung Sung, Jihoon Kim and Inkyu Lee [7]

In this paper, a method is introduced to improve the performance of the four transmit antenna quasi-orthogonal space-time block code (STBC) in the coded system. For the four transmit antenna case, the quasi-orthogonal STBC consists of two symbol groups which are orthogonal to each other, but intra group symbols are not. In uncoded system with the matched filter detection, constellation rotation can improve the performance. However, in coded systems, its gain is absorbed by the coding gain especially for lower rate code. An iterative decoding method [7] is introduced to improve the performance of quasi-orthogonal codes in coded systems. With conventional quasi-orthogonal STBC detection, the joint ML

detection can be improved by iterative processing between the demapper and the decoder. Simulation results shows that the performance improvement is about 2dB at 1% frame error rate.

Minh-Tuan Le, Van-Su Pham, Linh Mai and Giwan Yoon [8]

This paper proposes a very low-complexity maximum likelihood (ML) detection algorithm based on QR decomposition [8] for the quasi-orthogonal space–time block code (QSTBC) with four transmit antennas, called the LC-ML decoder. The proposed algorithm enables the QSTBC to achieve ML performance with significant reduction in computational load for any high-level modulation scheme [6].

Erik G. Larsson, Petre Stoica and Jian Li [9]

Space-time coding (STC) schemes for communication systems employing multiple transmit and receive antennas have been attracting increased attention. In this paper, two interrelated problems: detection of space-time codes under various interference conditions and information transfer from the STC detector to an error-correcting channel decoder have been addressed. By taking a systematic maximum-likelihood (ML) approach [9] to the joint detection and decoding problem, it is shown that how to design optimal detectors and how to integrate them with a channel decoder. It has also been discussed various aspects of channel modeling for STC communication receivers. In particular, while many previous works on space-time coding assume that the channel is a stochastic quantity, it is found that a deterministic channel model can have some advantages for the receiver design.

Zhiqiang Liu, Georgios B. Giannakis, Sergio Barbarossa and Anna Scaglione [10]

Relying on block precoding, this paper develops generalized space–time coded multicarrier transceivers appropriate for wireless propagation over frequency-selective multipath channels. Multicarrier precoding [10] maps the frequency-selective channel into a set of flat fading subchannels, whereas space–time encoding/decoding facilitates equalization and achieves performance gains by exploiting the diversity available with multiple transmit antennas [1]. When channel state information is unknown at the receiver, it is acquired blindly based on a deterministic variant of the constant-modulus algorithm that exploits the structure of space–time block codes.

Huseyin Arslan, Leonid Krasny, David Koilpillai and Sandeep Chennakeshu [11]

In this paper, efficient and practical approaches for Doppler spread estimation [11] in wireless mobile radio systems are described. A Hypothesis-testing approach, given the channel autocorrelation estimate, is utilized for Doppler spread estimation. The channel autocorrelation is estimated slot-by-slot using the knowledge of the channel estimates over the known fields of a TDMA burst, and averaged over several slots to reduce the effect of noise. In practical systems, the Doppler spread must be estimated in the presence of frequency offsets [12] between the transmitter and the receiver. Hence, an algorithm that decouples Doppler spread estimation from automatic frequency compensation (AFC) is also presented. In addition to the mean estimation error performance, the convergence and the tracking ability of the algorithms are evaluated via simulation using ANSI 136 Rev-B modulation and signal transmission format.

Trym H. Eggen, James C. Preisig and Arthur B. Baggeroer [12]

A receiver for coherent communication through underwater communication channels is analyzed. The receiver performance and stability versus delay spread, Doppler spread, and signal-to-noise ratio is quantified [12]. The stability is governed by the ill-conditioning of a correlation matrix estimate and it sets the limit on how many taps should be used for a channel with a given number of degrees of freedom.

Lu Qiaoli, Chen Wei, Xie Tao and Long Biqi [13]

In this paper, an efficient and practical design for Doppler spread estimation in mobile OFDM systems is described. A channel auto-correlation function algorithm is proposed for Doppler spread estimation [13]. The Doppler spread estimator is based on finding the auto-correlation function of time domain channel estimates over several OFDM symbols. The estimation performance of the estimator is evaluated via computer simulation using national standard digital television system DTMB signal transmission format. Simulation results show that the proposed Doppler spread estimator can provide high estimation accuracy [12] for a wide range of Doppler spread. Moreover, the proposed algorithm relies on periodic channel estimate and can also be applied into other OFDM systems with known pilot symbols inserted within the data fields.

Kuo-Hui Li and Mary Ann Ingram [14]

A beamforming network [14] is considered for a space–time block-coded orthogonal frequency-division multiplexing system in a high-speed indoor wireless network. It is found that choosing the most powerful beams for transmission provide the best performance in the absence of interference. In the presence of interference, an iterative two-metric beam-selection method is proposed [14].

Jaeho Chug, Jaehwa Kim, Taekon Kim and Jaemoon Jo [15]

In this paper, the simulation results for the bit error rate performance of Multi-Input Multi- Output (MIMO) [15] systems supporting 96 Mbps data-rate based on *IEEE* 802.11a *OFDM PHY* layer under various channel models have been shown. Spatial multiplexing system combined with space-time trellis coding (SM-STTC) [2] undergoes the most significant performance degradation in correlated channel environments compared to that in an uncorrelated channel. Spatial multiplexing system combined with space time block coding (SM-STBC) and hybrid SM-STBC system produce similar results in correlated fading channels. *V-BLAST* system achieves comparable performance to other systems under correlated channels when receiver diversity is exploited.

Enis Akay and Ender Ayanoglu [16]

In addition to the destructive multipath nature of wireless channels, frequency selective channels impose intersymbol interference (ISI) while offering frequency diversity for successfully designed systems. Orthogonal frequency division multiplexing (OFDM) has been shown to combat ISI extremely well by converting the frequency selective channel into parallel flat fading channels. On the other hand, bit interleaved coded modulation (BICM)[16] was shown to have high performance for flat fading Rayleigh channels. Combination of BICM and OFDM was shown to exploit the diversity that is inherited within the frequency selective fading channels. In other words, BICM-OFDM is a very effective technique to provide diversity gain, employing frequency diversity. Orthogonal space-time block codes (STBC) make use of diversity in the space domain by coding in space and time. Thus, by combining BICM-OFDM and STBC, diversity in frequency and space can be taken advantage of. In this paper we show and quantify both analytically and via simulations that for frequency selective fading channels, BICM-STBC-OFDM systems can fully and successfully exploit the frequency and space diversity to the maximum available extent.

Zhuo Chen, Zhanjiang Chi, Yonghui Li, Branka Vucetic and Hajime Suzuki [17]

In this paper, the error performance of an uncoded multiple-input-multiple-output (MIMO) scheme combining single transmit antenna selection and receiver maximal-ratio combining (the TAS/MRC scheme)[17] is investigated for flat Nakagami-m fading channels with arbitrary values of m $\geq 1/2$. The exact symbol error rate (SER) expressions are developed based on the moment generating function (MGF) [18] method for M-ary phase-shift keying (M-PSK) and M-ary quadrature amplitude modulation (M-QAM). The asymptotic SER analysis reveals a diversity order equal to the product of the m parameter, the number of transmit antennas and the number of receive antennas. Theoretic analysis is verified by simulation. These analytical results quantify the impact of the fading severity on the system performance, and provide guidance for system design

Yu Zhang and Huaping Liu [18]

In this paper, it has been studied the impact of time-selective fading on quasi-orthogonal space-time (ST)[18] coded orthogonal frequency-division multiplexing (OFDM) systems over frequency-selective Rayleigh fading channels. OFDM is robust against frequency-selective fading, but it is more vulnerable to time-selective fading than single-carrier systems. In ST-OFDM, channel time variations cause not only intercarrier interference among different subcarriers in one OFDM symbol, but also intertransmit-antenna interference. It has been quantified the impact of time-selective fading on the performance of quasi-orthogonal ST-OFDM systems by deriving, via an analytical approach, the expressions of carrier-to-interference and signal-to-interference-plus-noise ratios. It has been observed that system error performance is insensitive to changes in vehicle speeds and the channel power-delay profile, but very sensitive to changes in the number of subcarriers. It has also been evaluated the performance of five different detection schemes in the presence of time-selective fading. It has been shown that although there exist differences in their relative performances, all these detection schemes suffer from an irreducible error floor [15].

CHAPTER 3

INTRODUCTION TO OFDM WIRELESS COMMUNICATION SYSTEMS

3.1 Basics

FDMA technique is used to increase the data transmission rate by simultaneously sending different signals through various channels comparatively of small bandwidth irrespective of large bandwidth channel .small bandwidth channel results following advantages.

1) It converts frequency selective fading into flat fading results in B << Bc (coherence bandwidth). Hence, single-tape equalizer is required at the receiver end to compensate the effect of multipath fading channel.
2) Impulse noise effect decrease because of less power contribution to a particular channel. Noise power spreads in the whole frequency spectrum.

Due to higher transmission rate, time delay and time spread, ISI and ICI should be reduced. It can be done by making the signals orthogonal in time domain, which results in 50% overlapping in bandwidth, hence, there is saving in bandwidth as well. OFDM is simply defined as a form of multi-carrier modulation, where the carrier spacing is carefully selected so that each sub carrier is orthogonal to the other sub carriers. Since, the carriers are orthogonal to each other, the nulls of one carrier coincides with the peak of another sub-carrier. As a result, it is possible to extract the sub carrier of interest.

In OFDM, there are large number of narrowband sub-channels exist. The frequency range between carriers is carefully chosen in order to make them orthogonal to one another. In fact, the carriers are separated by an interval of 1/T, where T represents the duration of an OFDM symbol. The frequency spectrum of an OFDM transmission is illustrated in fig. 3.1. Each sinc waveform of the frequency spectrum is shown in Fig. 3.1.

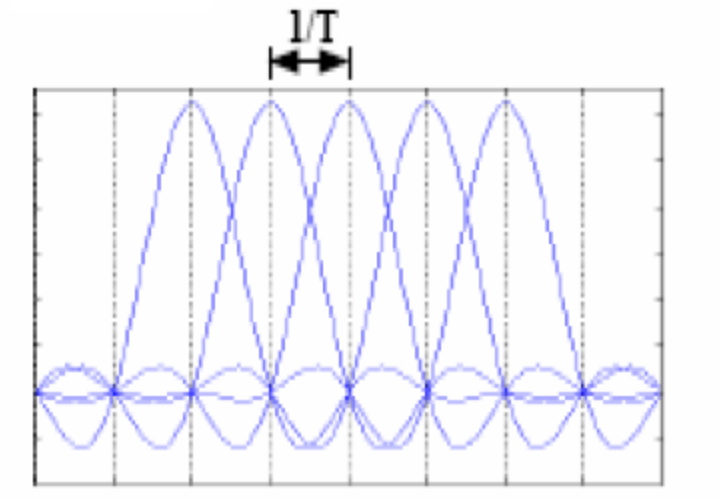

Fig 3.1 *OFDM representation in frequency domain [19]*

One could easily notice that the frequency spectrum of one carrier exhibits zero-crossing at central frequencies corresponding to all other carriers. At these frequencies, the inter carrier interference is eliminated, although the individual spectra of subcarriers overlap. It is well known that the orthogonal signals can be separated at the receiver by correlation techniques. The receiver acts as a bank of demodulators, translating each carrier down to baseband, the resulting signal then being integrated over a symbol period to recover the data. The waveform of some carriers in an OFDM transmission is illustrated in Fig. 3.1. The Fig. 3.1 indicates the spectrum of carriers significantly overlaps over the other carrier. This is contrary to the traditional FDMA technique in which a guard band is provided between each carrier. From the Fig. 3.1 illustrated, it is clear that OFDM is a highly efficient system and hence is often regarded as the optimal version of multi-carrier transmission schemes. The number of sub channels transmitted is fairly arbitrary with certain broad constraints, but in practical systems, sub channels tend to be extremely numerous and close to each other.

3.2 Block Diagram of OFDM System using FFT

The input data sequence is baseband modulated, obtained by using a digital modulation scheme. Various modulation schemes could be employed such as BPSK, QPSK

(also with their differential form) and QAM with several different signal constellations. There are also forms of OFDM where a distinct modulation on each sub channel is performed (e.g. transmitting more bits using an adequate modulation method on the carriers that are more„ confident", like in ADSL systems). The modulation is performed on each parallel sub stream, that is on the symbols belonging to adjacent DFT frames. The data symbols are parallelized in N different sub-streams.

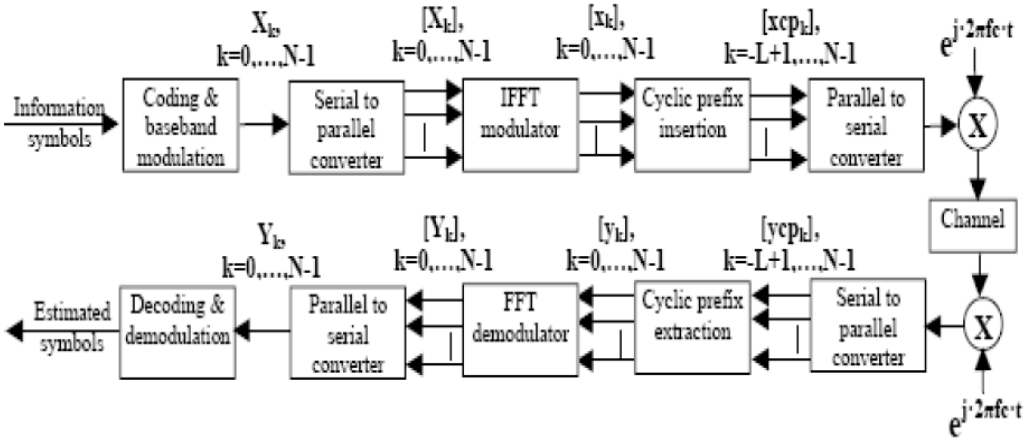

Fig. 3.2 *OFDM implementation using FFT method [23]*

Each sub-stream will modulate a separate carrier through the IFFT modulation block, which is in fact the key element of an OFDM scheme, as we will see later. A cyclic prefix [14] is inserted in order to eliminate the inter symbol and inter-block interference (IBI). This cyclic prefix of length L is a circular extension of the IFFT-modulated symbol, obtained by copying the last L samples of the symbol in front of it. IDFT operation is performed on data symbols, resulting in forming an OFDM symbol that will modulate a high-frequency carrier before its transmission through the channel. The radio channel is generally referred as a linear time-variant system. At the receiver, the inverse operations are performed. The data are down-converted to the baseband and the cyclic prefix is removed. The coherent FFT demodulator will ideally retrieve the exact form of transmitted symbols. The data is converted into serial mode and the appropriated demodulation scheme will be used to estimate the transmitted symbols. In this section, the key points of OFDM are presented: the principles of a multicarrier (parallel) transmission, the usage of FFT and the cyclic prefix [19].

3.3 Problems in OFDM Systems

There are some obstacles in using OFDM in transmission system in contrast to its advantages.

1) High PAPR

A major obstacle is that the OFDM signal exhibits a very high Peak to Average Power Ratio (PAPR)[19]. Therefore, RF power amplifiers should be operated in a very large linear region. Otherwise, the signal peaks get into non-linear region of the power amplifier, causing signal distortion. This signal distortion introduces inter modulation among the subcarriers. Thus, the power amplifiers should be operated with large power back-offs. On the other hand, this leads to very inefficient amplification and expensive transmitters. Thus, it is highly desirable to reduce the PAPR. The other limitation of OFDM in many applications is that it is very sensitive to frequency errors [19], caused by frequency differences between the local oscillators in the transmitter and the receiver. Carrier frequency offset causes a number of impairments including attenuation and rotation of each of the subcarriers and inter-carrier interference (ICI) between subcarriers.

2) Frequency Offset

In the mobile radio environment, the relative movement between transmitter and receiver causes Doppler frequency shifts, in addition, the carriers can never be perfectly synchronized. These random frequency errors in OFDM system distort orthogonality between subcarriers and thus intercarrier interference (ICI) occurs. A Number of methods have been developed to reduce this sensitivity to frequency offset [19].

OFDM has several properties, which make it an attractive modulation scheme for high speed transmission links. However, one major difficulty is its large Peak to Average Power Ratio (PAPR). These large peaks cause saturation in power amplifiers, leading to intermodulation among the subcarriers and disturbing out of band energy. Therefore, it is desirable to reduce the PAPR. To reduce the PAPR, several techniques have been proposed such as clipping, coding, peak windowing, Tone Reservation and Tone Injection. But, most of these methods are unable to achieve simultaneously a large reduction in PAPR with low

complexity, with low coding overhead, without performance degradation and without transmitter receiver symbol handshake.

3.4 Symbol Synchronization

The objective here is to know when the symbol starts. A timing offset gives rise to a phase rotation of the subcarriers. This phase rotation is largest on the edges of the frequency band. If a timing error is small enough to keep the channel impulse response within the cyclic prefix, the orthogonality is maintained. In this case, the symbol timing delay can be viewed as a phase shift introduced by the channel and the phase rotations can be estimated by a channel estimator. If a time shift is larger than the cyclic prefix, ISI will occur. There are two main methods for timing synchronization, based on pilots or on the cyclic prefix.

3.4.1 Pilots

In this scheme [21], two symbols with identical data are used to estimate the frequency offset. Moose's work [22] is the basis for the Schmidl method. He derived a maximum likelihood estimator to detect the carrier frequency offset that is calculated after the FFT in the frequency domain. The estimation technique involves repetition of data symbols and comparison of the phases of each of the carriers between the successive symbols. Since the modulation phase values are not changed, the phase shift of each of the carriers between the successive repeated symbols is due to the frequency offset and noise. The acquisition range in the Schmidl method is limited to ±1/2 of the carrier spacing and it is assumed that the symbol timing was estimated perfectly.

In this sense, this method also falls under the carrier synchronization category. However, it is included in the symbol synchronization category because[19], it also provides a method of symbol synchronization not using a cyclic prefix. In the paper by Schmidl, a method is presented to perform rapid synchronization with a relatively simplified computation in the time domain and an extended range for the acquisition of the carrier frequency offset. The algorithm presented here is suitable for continuous transmission (as in broadcasting) and for burst transmission (as in wireless LAN applications). The synchronization is performed on a training sequence of two OFDM symbols. The frame

timing is performed using one unique OFDM symbol as the first symbol, which has a repetition within half a symbol period. In the burst mode this is very effective in determining the start of a burst of data.

The symbol timing recovery relies on searching for a training symbol with two identical halves in time domain, with the crucial assumption that the channel effects are identical, except that there will be a phase difference between them caused by the carrier frequency offset. The two halves of the training symbol are made identical by transmitting a PN sequence on the even subcarriers while zeros are inserted on the odd ones. In this way, the receiver can distinguish between symbols meant for synchronization and symbols that contain data. The transmitted data will not be mistaken as the start of the frame since the data symbol must contain data on the odd frequencies.

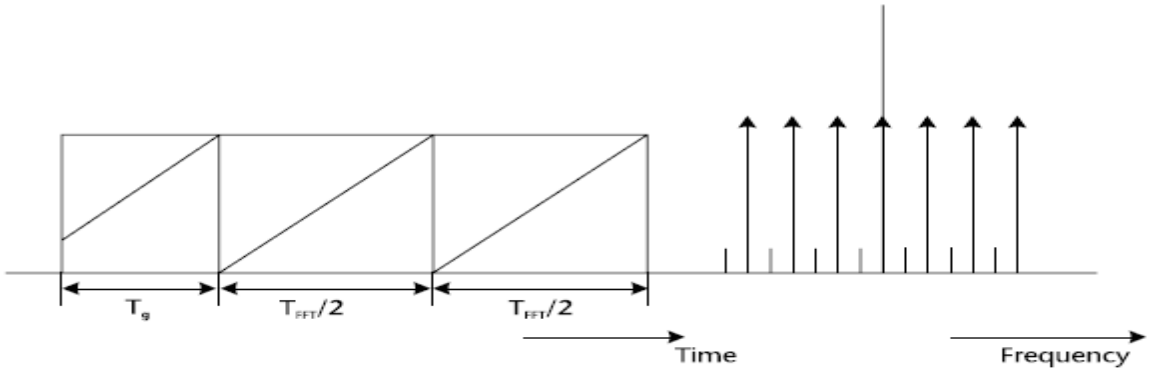

Fig 3.3 *Training symbol with two identical halves in time domain resulting in nulls in odd frequencies in frequency domain[19]*

The first half of the training symbol is considered to be identical to the second half, after passing through the channel, except for the progressive phase shift caused by the frequency offset. By multiplying the conjugate of the sample from the first half with the corresponding sample from the second half (T /2 seconds later), the arbitrary phases of the OFDM signal and the effect of the channel should cancel out. As a result, only the phase difference will remain, which can be used as an estimate for the frequency offset f_d. The phase difference is constant because the length between the samples (L) is constant. At the start of the frame, the products of each pair of samples will have approximately the same

phase, so the magnitude of the sum will have a large value (like constructive interference). The sum of products can be expressed in the following equation:

$$P(d) = \sum_{m=0}^{L-1} (r_{d+m}^{*} . r_{d+m+L}) \quad (3.1)$$

where $L = N_{FFT}/2$.

The sum of the correlation value is normalized with the received energy from the second half of the first training sequence. This energy is calculated as,

$$P(d) = \sum_{m=0}^{L-1} r_{d++m+L}^{2} \quad (3.2)$$

The maximum value will be reached as soon as the samples are pairs with distances of half a symbol period. This will result in Fig. 3.4 with a plateau of length equal to the guard interval. When the signal is propagating over a realistic channel, with multipath fading, the length of this plateau will be shortened by the length of the channel delay time. The maximum value will be reached as soon as the samples are pairs with distances of half a symbol period. This will result in Fig. 3.4 with a plateau of length equal to the guard interval.

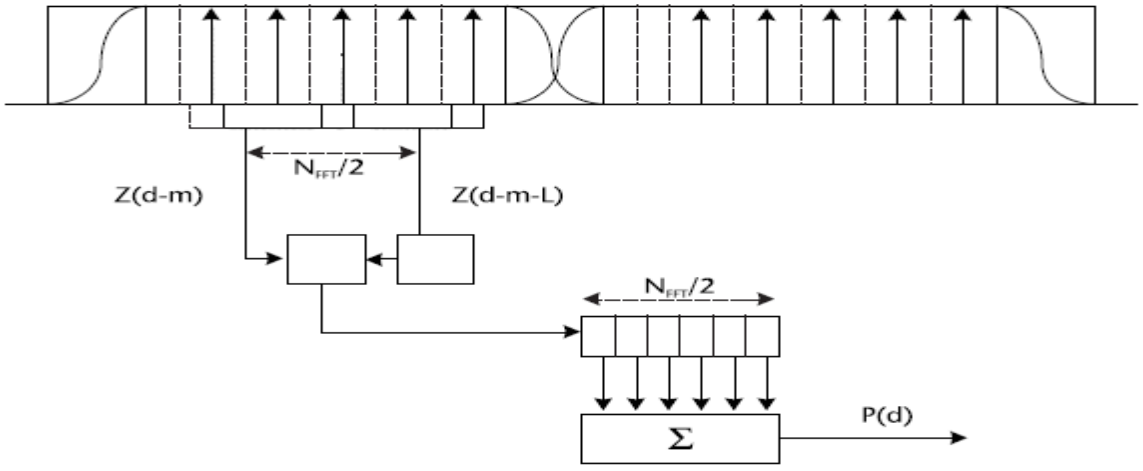

Fig 3.4 *Computation of symbol timing estimation[19]*

The maximum value will be reached as soon as the samples are pairs with distances of half a symbol period. This will result in a figure with a plateau of length equal to the guard interval. When the signal is propagating over a realistic channel, with multipath fading, the length of this plateau will be shortened by the length of the channel delay time.

The start of the frame can be taken anywhere on this plateau, as it will always be a ‘‘rough’’ estimation of the symbol timing error. The symbol timing error will have little effect as long as that part of the guard interval (GI) is discarded, which is corrupted by ISI. The carrier frequency offset is estimated in two steps. First, the fractional part is detected and compensated for. Then the integer part is estimated and corrected.

3.5 Carrier Synchronization

Frequency offsets are created by differences in oscillators in transmitter and receiver, Doppler shifts, or phase noise introduced by nonlinear channels. There are two destructive effects caused by a carrier frequency offset in OFDM systems. One is the reduction of signal amplitude (the sinc functions are shifted and no longer sampled at the peak) and the other is the introduction of ICI from other carriers. The latter is caused by the loss of orthogonality between the subchannels. Similar to symbol synchronization, carrier synchronization can also be divided into two categories: based on pilots or on the cyclic prefix.

3.5.1 Pilots

This approach has been addressed in [11]. Here, the subcarriers are used for the transmission of pilots (usually a PN sequence). Using these known symbols, the phase rotations caused by the frequency offset can be estimated. Under the assumption that the frequency offset is less than half the subcarrier spacing, there is a one-to-one correspondence between the phase rotations and the frequency offset. To assure this, an algorithm is constructed by forming a function, which is sinc shaped and has a peak for $f - f' = 0$. It was found that by evaluating this function in points $0.1/T$ apart, an acquisition can be obtained by maximizing that function. This was found to work well both for an AWGN channel and a fading channel.

3.5.2 Cyclic Prefix

The redundancy of the cyclic prefix can be used in several ways (e.g., by creating a function that peaks at zero offset and finding its maximizing value or by doing maximum likelihood estimation, as previously discussed). If the frequency error is slowly varying compared with the OFDM symbol rate, a phase-locked loop (PLL) can be used to further reduce the error.

3.6 Sampling-Frequency Synchronization

The received continuous-time signal is sampled at instants determined by the receiver clock. There are two methods to deal with the mismatch in sampling frequency. In synchronized-sampling systems, a timing algorithm controls a voltage controlled crystal oscillator to align the receiver clock with the transmitter clock. The other method is non-synchronized sampling, where the sampling rate remains fixed, which requires post processing in the digital domain. The effect of clock frequency offset is two-fold: the useful signal component is rotated and attenuated and, in addition, ICI is introduced. The BER performance of a non-synchronized OFDM system has been investigated.

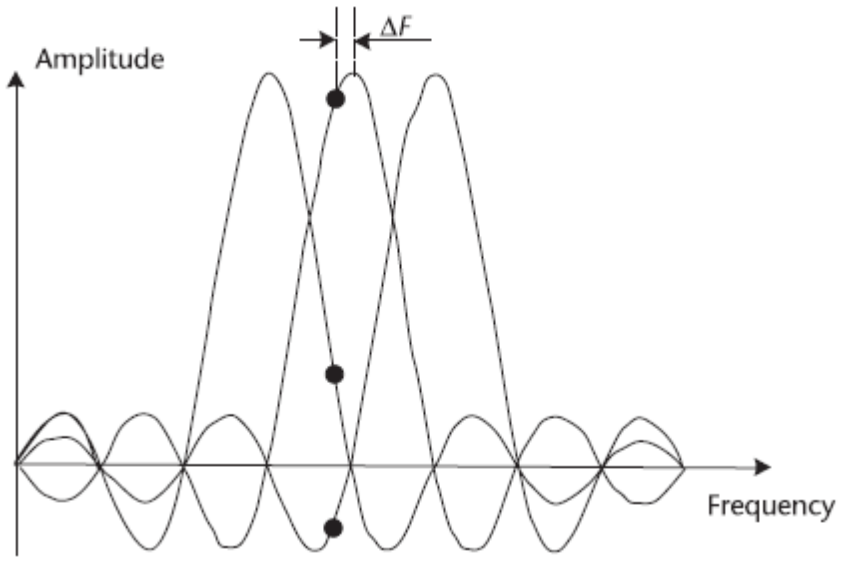

Fig 3.5 *The carrier synchronization problem[19]*

It is shown that non-synchronized sampling is much more sensitive to a frequency offset, compared with a synchronized- sampling system. For non-synchronized sampling systems, it is shown that the degradation (in dB) due to a frequency sampling offset depends on the square of the carrier index and on the square of the relative frequency offset.

CHAPTER 4

INTRODUCTION TO FADING IN WIRELESS SYSTEM

Attenuation is the drop in the signal power when signal is transmitted from one point to another. It can be caused by the transmission path length, obstructions in the signal path, and multipath effects. Any object, which obstructs the line of sight of signal from the transmitter to the receiver, can cause attenuation. Shadowing of the signal can occur whenever there is an obstruction between the transmitter and receiver. It is generally caused by the buildings and hills, and is the most important environmental attenuation factor. Shadowing is most severe in heavily built up areas, due to the obstruction of signal from the buildings. However, hills can cause a large problem due to the large shadow, they produce. Radio signals diffract off the boundaries of obstructions, thus preventing total shadowing of the signals behind hills and buildings. However, the amount of diffraction is dependent on the radio frequency used. Thus high frequency signals, especially, Ultra High Frequencies (UHF) and microwave signals require line of sight for adequate signal strength. To overcome the problem of shadowing, transmitters are usually elevated as high as possible to minimize the number of obstructions. Typical amounts of variation in attenuation due to shadowing are shown in Table 4.1. Here typical attenuation due to shadowing in heavy built up urban center, sub-urban area, open rural area and terrain irregularities is shown.

Typical Attenuation in a radio channel

Table 4.1 [23]

Description	Typical Attenuation due to Shadowing
Heavy built-up urban center	20dB variation from street to street
Sub-Urban area (fewer large buildings)	10dB greater signal power than built up urban center
Open rural area	20dB greater signal power than sub-urban areas
Terrain irregularities and tree foliage	3-12dB signal power variation

Shadowed areas tend to be large, resulting in the rate of change of the signal power being slow. For this reason, it is termed slow-fading or log-normal shadowing**.**

4.1 Mobile Radio Propagation

Fading effects that characterize the mobile communication can be of two types: **large-scale** and **small-scale fading**. Large-scale fading represents the average signal power attenuation or path loss due to motion over large areas. This phenomenon is affected by prominent terrain contours (hills, forests, billboards, clumps of buildings etc.) between the transmitter and the receiver. The receiver is often represented as being "shadowed" by such prominences. This is described in terms of a log-normally distributed variation [24] about the mean. Small-scale fading refers to the dramatic changes in signal amplitude and phase that can be experienced as a result of small changes (as small as the half-wavelength) in the spatial separation between a receiver and transmitter. Small scale fading often described by Rayleigh fading, if the multiple reflective paths are large in number and there is no line-of-sight between the transmitter and the receiver. When there is a dominant fading signal component present, such as a line-of sight propagation path, the small scale fading envelope is described by a Rician PDF.

4.1.1 Multi-Path Spread

In conventional wireless communication systems, one antenna is used at the source and another antenna is used at the destination as the receiver. As we discussed, this structure sometimes gives rise to problems of multipath effects. When an electromagnetic field meets with the obstructions such as hills, canyons, buildings and utility wires, the wave fronts are scattered, and thus they take many paths to reach the receiver. In digital communication systems, such as wireless internet, multi-path fading can cause reduction in data speed and increase in the number of errors. We illustrate the effects of the scattered wave from the transmitter to the receiver, causing the multi-path effect, resulting in signal distortion and delay, that can not be ignored.

4.1.2 Flat and Frequency Selective Fading

There are generally two types of fading, namely, flat fading and frequency selective fading, when signals are transmitted from the transmitter to the receivers. If all the spectral components of the transmitted signals are affected by the same amplitude gains and phase shifts, the channel is called flat fading channel. In this case, the transmitted signal bandwidth is much smaller than the channel's coherence bandwidth. Flat fading channel is encountered in wireless environment and causes deep fades. The amplitude distribution of flat fading is either Rayleigh distribution or Rician distribution.

On the other hand, if the spectral components of the transmitted signals are affected by different amplitude gains and phase shifts, the fading is said to be frequency selective. In this case, the transmitted bandwidth is larger than the channel's coherence bandwidth. Frequency selective fading will induce inter-symbol interference, which results in signal distortion. Assuming a single is transmitted, whose time duration *Tm* is the duration between the first and last received component, that possesses the maximum delay spread, therefore the coherence bandwidth *fc* is 1/ *Tm.* Let the symbol period is *Ts.* A channel is said to be frequency selective fading if $Tm>Ts$, and it is said to be flat fading if $Tm<Ts$.

In radio transmission, the channel spectral response is not flat. It has dips or fades due to reflections, causing cancellation of certain frequencies at the receiver. Reflections from near-by objects (e.g. ground, buildings, trees, etc) can lead to multipath signals of same signal power as the direct signal. This can result in deep nulls in the received signal power due to destructive interference. For narrow bandwidth transmission, if the null in the frequency response occurs at the transmission frequency, then the entire signal can be lost. This can be partly overcome in two ways. By transmitting a wide wideband signal or spread spectrum as CDMA, any dips in the spectrum only result in a small loss of signal power, rather than a complete loss. Another method is to split the whole frequency spectrum into many frequency channels of small bandwidth, as is done in a COFDM/OFDM transmission. The original signal is spread over a wide bandwidth, thus any null in the spectrum is unlikely to occur at all of the carrier frequencies. This will result in only some of the carriers being lost, rather than the entire signal. The information in the lost carriers can be recovered provided enough FEC (forward error control).

4.1.3 Delay Spread:

The received radio signal from a transmitter consists of typically a direct signal, plus reflected signals from the objects such as buildings, mountains and other structures. The reflected signals arrive at a later time than the direct signal because of the extra path length, giving rise to a slightly different arrival time of the transmitted pulse, thus spreading the received energy. Delay spread is the time spread between the arrival of the first and last multipath signal seen by the receiver. In a digital system, the delay spread can lead to inter-symbol interference. This is due to the overlapping of original signal with the multipath signals. This can cause significant errors in high bit rate systems, especially when using time division multiplexing (TDMA). Fig. 4.1 shows the effect of inter-symbol interference due to delay spread on the received signal. As the transmitted bit rate is increased, the amount of inter symbol interference also increases. The effect starts to become very significant when the delay spread is greater than approximately 50% of the bit time.

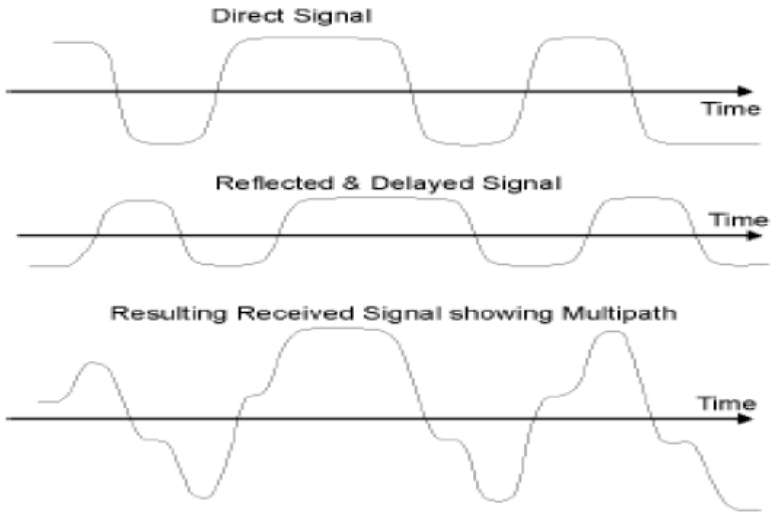

Fig. 4.1 Delay spread [23]

4.1.4 Doppler Shift

Another major concern in wireless communication, is the Doppler effect (shift). As we all know, this effect occurs due to the relative speed between the elements in the

communication system. The Doppler effect is the change in frequency/wavelength of a wave as perceived by an observer moving relative to the source of the waves. The total Doppler effect may therefore results from either motion of the source or motion of the observer. The Doppler shift is directly proportional to the magnitude of the relative speed [12] and is modeled here as a shifting to the carrier frequency.

For waves, which do not require a medium such as light, only the relative difference in velocity between the observer and the source needs to be considered. In wireless communication, when the electromagnetic wave is travelling towards or away from the receiver, the carrier frequency will be shifted, causing Doppler shift. It is noticed that the Doppler shift is usually prominent when the transmit antenna is far from receive antenna. The phase difference between two transmission paths is:

$$\Delta \phi = \frac{2\lambda \Delta l}{\lambda} = \frac{2\lambda v \Delta t}{\lambda} \cos\theta \tag{4.1}$$

The Doppler shift is

$$f_d = \frac{1}{2\pi} . \frac{\Delta \phi}{\Delta t} = \frac{v}{\lambda} cos\theta \tag{4.2}$$

where λ = the wavelength of signal, l = length between the source and the observer.

θ = angle between line (joining the source and the observer) and direction of motion

v = velocity of observer

The detected frequency increases as the objects moving toward the observer. Conversely, the detected frequency decreases when the source moves away, and so the source's velocity is added when the motion is away.

If a pure sinusoid is transmitted, a range of frequencies adjacent to the frequency of sinusoid will be received. Doppler shift broadens the spectrum of the received signal by spreading the basic spectrum in frequency domain.

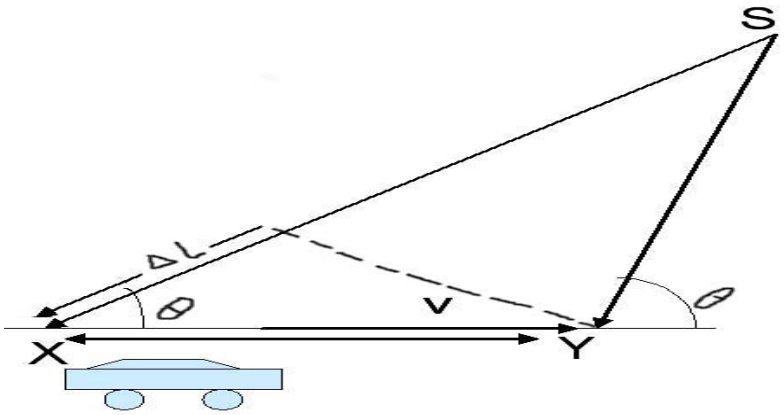

Fig 4.2 Doppler shift due to receiver velocity [23]

If the signal spectrum is wide enough compared to this spreading, the effect is not noticeable. Let us investigate the BPSK signals in slow, Rayleigh and Doppler fading channel with additive white Gaussian noise for one transmit antenna and one receive antenna. One can see that when f_d is larger, the performance is getting worse because of the effect of Doppler shift. Both multi-path fading and Doppler effects can impair the reception of the transmitted signal. It is also well known that the inter-symbol interference happens when signals via multiple paths are received with various delays and co-channel users create distortion to the target user.

Diversity is an effective way, to improve the error rate performance in fading channels. MIMO OFDM is introduce in wireless communication to offer diversity, capacity and array gain by using MIMO and also to avoid inter symbol interference by using OFDM.

4.1.5 Slow and Fast Fading

Fading due to Doppler spread includes both slow fading and fast fading. In wireless communication, a channel can be time-varying and this dynamic channel is characterized as slow or fast fading channel. Fast fading channel changes significantly during the symbol period. When the channel varies rapidly, it distorts the symbol's amplitude and phase erratically over its interval. On the other hand, slow fading occurs when the channel changes much slower than one symbol duration. This does not imply that the effects of the channel

can be neglected, but it is possible to track the changes in the channel appropriately to compensate the channel dynamics.

We define coherence time T_c of the channel as the period of time over which the channel gain remains constant. T_c is closely related to Doppler spread f_d as :

$$T_c \approx 1/ f_d$$

If the symbol time duration T_s is smaller than T_c , the fading is slow fading, otherwise the channel fading is fast fading.

4.2 Multi-Path Fading Model

The following fading models are described here in multipath fading environment.

4.2.1 Rayleigh Fading

Rayleigh fading is a statistical model for the effect of a propagation environment on a radio signal. Rayleigh fading models assume that the magnitude of a signal that has passed through such a transmission medium (also called a communications channel) will vary randomly, or fade, according to a Rayleigh distribution (the radial component of the sum of two uncorrelated Gaussian random variables). Rayleigh fading is viewed as a reasonable model for tropospheric, ionospheric signal propagation and for the effect of heavily built-up urban environment on radio signals. Rayleigh fading is most applicable when there is no dominant propagation along a line of sight between the transmitter and the receiver. Rayleigh fading is a reasonable model when there are many objects in the environment, those scatter the radio signal before it arrives at the receiver. The central limit theorem holds that, if there is sufficiently much scattering, the channel impulse response will be modeled as a Gaussian process irrespective of the distribution of the individual components. The probability density function of Rayleigh channel [24] is :

$$f(r) = \frac{r}{\Omega^2} \exp\left(\frac{-r^2}{2\Omega^2}\right) , \; r \geq 0 \qquad (4.3)$$

Where r is the amplitude of the envelope and Ω is the variance.

4.2.2 Rician Fading

When there is one or more dominant paths exist between transmitter and receiver, the channel response is described by Rician distribution. The Rician distribution is given by

$$f(r) = \frac{r}{\Omega^2} \exp\left(\frac{-r^2+A^2}{2\Omega^2}\right) I(Ar/\Omega^2),\ r \geq 0 \tag{4.4}$$

Where A denotes the peak amplitude of the dominant signal, is the modified Bessel function of first kind and zero order.

4.2.3 Nakagami-m Fading

Both Rayleigh and Rician distributions are frequently used to describe the statistical flucations of signals received via multipath fading channel. Another distribution that is frequently used is Nakagami-m distribution. PDF of Nakagami-m distribution is given by

$$P_R(r) = \frac{2}{\Gamma(m)} \left(\frac{m}{\Omega}\right)^m r^{2m-1} e^{-mr^2/\Omega} \tag{4.5}$$

Where Ω is defined as $\Omega = E(R^2)$

Parameter m is defined as the ratio of moments, called the fading figure.

$$m = \frac{\Omega^2}{E[(R^2-\Omega)^2]}, \quad m \geq \frac{1}{2} \tag{4.6}$$

When m=1, it becomes Rayleigh distribution. With the increase in value of m, the BER decreases.

CHAPTER 5

SPACE –TIME BLOCK-CODES

5.1 Diversity

In telecommunication, diversity scheme refers to a method for improving the reliability of a message signal by using two or more communication channels with different characteristics. Diversity plays an important role in combating fading, co-channel interference and avoiding error bursts. It is based on the fact that the individual channels experience different levels of fading and interference. Multiple versions of the same signal may be transmitted and/or received and combined in the receiver. Alternatively, a redundant forward error correction code may be added and multiple copies of the message transmitted over different channels. Diversity techniques may exploit the multipath propagation effects, resulting in a diversity gain, often measured in decibels.

The following classes of diversity schemes can be identified:

- **Time diversity**: Multiple versions of the same signal are transmitted at different time instants. Alternatively, a redundant forward error correction code is added and the message is spread in time by means of bit-interleaving before it is transmitted. Thus, error bursts are avoided, which simplifies the error correction.
- **Frequency diversity**: The signal is transmitted using several frequency channels or spread over a wide spectrum that is affected by frequency-selective fading. Middle-late 20th century microwave radio relay lines often used several regular wideband radio channels, and one protection channel for automatic use by any faded channel.
- **Space diversity**: The signal is transmitted over several different propagation paths. In the case of wired transmission, this can be achieved by transmitting via multiple wires. In the case of wireless transmission, it can be achieved by antenna diversity using multiple transmitter antennas (transmit diversity) and/or multiple receiving antennas (receiver diversity). In the latter case, a diversity combining technique is applied before further signal processing takes place. If the antennas are far apart, for example at different cellular base station sites or WLAN access points, this is called

macro diversity or site diversity. If the antennas are at a distance in the order of one wavelength, this is called micro diversity. A special case is phased antenna arrays, which also can be used for beamforming, MIMO channels and Space–time coding (STC).

- **Polarization diversity**: Multiple versions of a signal are transmitted and received via antennas with different polarization. A diversity combining technique is applied on the receiver side.

Space–time block coding is a technique used to improve the performance of a wireless communication system, where the receiver is provided with multiple signals propagating via different paths. The **space–time code** (STC) [2] is a method employed to improve the reliability of data transmission in wireless communication systems using multiple transmit antennas STCs rely on transmitting multiple, redundant copies of a data stream to the receiver in the hope that at least some of them may survive in the physical path between transmission and reception in a good enough state to allow reliable decoding.

Space time codes may be split into two main types:

- Space–time trellis codes (STTCs) distribute a trellis code over multiple antennas and multiple time-slots and provide both coding gain and diversity gain.
- Space–time block codes (STBCs) act on a block of data at once (similarly to block codes) and provide only diversity gain, but are much less complex in implementation terms than STTCs.

STC may be further subdivided according to whether the receiver knows the channel impairments. In coherent STC, the receiver knows the channel impairments through training or some other form of estimation. These codes have been studied more widely because they are less complex than their non-coherent counterparts. In non-coherent STC the receiver does not know the channel impairments, but knows the statistics of the channel. In differential space–time codes, neither the channel nor the statistics of the channel is available.

The concept behind space-time block coding is to transmit multiple copies of the same data through multiple antennas in order to improve the reliability of the data-transfer through the noisy channel.

5.2 Space-Time Block Code (STBC)

The very first and well-known STBC is the Alamouti code [1], which is a complex orthogonal space-time code specialized for the case of two transmit antennas . In this section, we first consider the Alamouti space-time coding technique and then, its generalization to the case of three antennas or more.

5.2.1 Alamouti Space-Time Code

A complex orthogonal space-time block code for two transmit antennas was developed by Alamouti. In the Alamouti encoder, two consecutive symbols x_1 and x_2 are encoded with the following space-time codeword matrix:

$$\mathbf{X} = \begin{bmatrix} x_1 & -x_2^* \\ x_2 & x_1^* \end{bmatrix} \tag{5.1}$$

Alamouti encoded signal is transmitted from the two transmit antennas over two symbol periods. During the first symbol period, two symbols x_1 and x_2 are simultaneously transmitted from the two transmit antennas. During the second symbol period, these symbols are transmitted again, where $-x_2^*$ is transmitted from the first transmit antenna and x_1^* transmitted from the second transmit antenna.

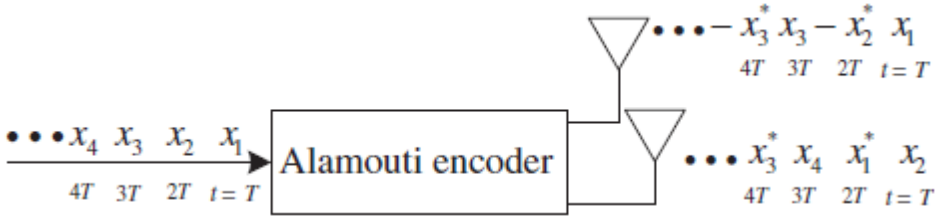

Fig 5.1 Alamouti encoder[24]

Note that the Alamouti codeword X is a complex-orthogonal matrix, that is,

$$\mathbf{X}\mathbf{X}^{\boldsymbol{H}} = \begin{bmatrix} |x_1|^2+|x_2|^2 & 0 \\ 0 & |x_1|^2+|x_2|^2 \end{bmatrix} = (|x_1|^2 + |x_2|^2)\mathrm{I}_2 \tag{5.2}$$

where I_2 denotes the 2x2 identity matrix. The transmission rate of Alamouti code is unity.

Consider two different Alamouti codes,

$$\mathbf{X}p = \begin{bmatrix} x_{1,p} & -x_{2,p}^* \\ x_{2,p} & x_{1,p}^* \end{bmatrix} \quad \text{and} \quad \mathrm{X}q = \begin{bmatrix} x_{1,q} & -x_{2,q}^* \\ x_{2,q} & x_{1,q}^* \end{bmatrix} \tag{5.3}$$

where $\left[x_{1,p}\ x_{2,p}\right]^T \neq \left[x_{1,q}\ x_{2,q}\right]^T$. Then the minimum rank is evaluated as

$$\begin{aligned} v &= \min_{p \neq q} \left\{ \begin{bmatrix} x_{1,p} & - & x_{1,q} & -x^*{}_{2,p} & + & x_{2,q}^* \\ x_{2,p} & - & x_{2,q} & x^*{}_{1,p} & - & x^*{}_{1,q} \end{bmatrix} \begin{bmatrix} x_{1,p} & - & x_{1,q} & -x^*{}_{2,p} & + & x_{2,q}^* \\ x_{2,p} & - & x_{2,q} & x^*{}_{1,p} & - & x^*{}_{1,q} \end{bmatrix}^H \right\} \\ &= \min_{p \neq q} \left\{ \begin{bmatrix} \mathrm{e}_1 & -\mathrm{e}_2^* \\ \mathrm{e}_2 & \mathrm{e}_1^* \end{bmatrix} \begin{bmatrix} \mathrm{e}_1^* & \mathrm{e}_2^* \\ -\mathrm{e}_2 & \mathrm{e}_1 \end{bmatrix} \right\} \\ &= \min_{p \neq q} \{(|e_1|^2 + |e_2|^2)\mathrm{I}_2\} \qquad (5.4) \\ &= 2 \end{aligned}$$

Note that e_1 and e_2 cannot be zeros simultaneously. The Alamouti code has been shown to have a diversity gain of 2. Note that the diversity analysis is based on ML signal detection at the receiver side. We now discuss ML signal detection for Alamouti space-time coding scheme. Here, we assume that two gains, h_1 and h_2, are time-invariant over two consecutive symbol periods, that is,

$$h_1(t) = h_1(t + T_s) = h_1 = |h_1|e^{j\theta_1} \tag{5.5}$$

$$\text{and} \quad h_2(t) = h_2(t + T_s) = h_2 = |h_2|e^{j\theta_2} \tag{5.6}$$

where $|h|$ and θ denote the amplitude gain and phase rotation over the symbol periods.

Let y_1 and y_2 denote the received signals at time t and t+Ts, respectively, then

$$y_1 = h_1 x_1 + h_2 x_2 + z_1 \tag{5.7}$$

$$y_2 = -h_1 x_2^* + h_2 x_1^* + z_2 \tag{5.8}$$

where z_1 and z_2 are the additive noise at time t and t+Ts, respectively. Taking complex conjugate of the second received signal, we have the following matrix vector equation:

$$\begin{bmatrix} y_1 \\ y_2^* \end{bmatrix} = \begin{bmatrix} h_1 & h_2 \\ h_2^* & -h_1^* \end{bmatrix} \begin{bmatrix} x_1 \\ x_2 \end{bmatrix} + \begin{bmatrix} z_1 \\ z_2^* \end{bmatrix} \tag{5.9}$$

In the course of time, from time t to t+Ts, the estimates for channels, h_1 and h_2 are provided by the channel estimator. In the following discussion, however, we assume an ideal

situation in which the channel gains, h_1 and h_2, are exactly known to the receiver. Then the transmit symbols are now two unknown variables in the above equation. Multiplying both sides of equation (5.9) by the Hermitian transpose of the channel matrix, that is,

$$\begin{bmatrix} h_1^* & h_2 \\ h_2^* & -h_1 \end{bmatrix} \begin{bmatrix} y_1 \\ y_2^* \end{bmatrix} = (|h_1|^2 + |h_2|^2) \begin{bmatrix} x_1 \\ x_2 \end{bmatrix} + \begin{bmatrix} h_1^* z_1 + h_2 z_1^* \\ h_2^* z_1 - h_1 z_1^* \end{bmatrix} \tag{5.10}$$

We note that other antenna interference does not exist anymore, that is, the unwanted symbol x_2 dropped out of y_1, while the unwanted symbol x_1 dropped out of y_2. This is attributed to complex orthogonality of the Alamouti code. This particular feature allows for simplification of the ML receiver structure as follows:

$$\hat{x}_{i,ML} = Q\left(\frac{\tilde{y}i}{|h_1|^2+|h_2|^2}\right), \; i = 1, 2. \tag{5.11}$$

where $Q(\cdot)$ denotes a slicing function that determines a transmit symbol for the given constellation set. The above equation (5.1) implies that x_1 and x_2 can be decided separately, which reduces the decoding complexity of original ML decoding algorithm.

5.2.2 Generalization of Space-Time Block-Coding

In the previous section, we have shown that, in case of Alamouti space-time code for two transmit antenna cases, ML decoding at the receiver can be implemented by simple linear processing. This idea was generalized for an arbitrary number of transmit antennas using the general orthogonal design method . Two main objectives of orthogonal space-time code design are to achieve the diversity order of N_T x N_R and to implement computationally efficient per-symbol detection at the receiver that achieves the ML performance.

The output of the space-time block encoder is a codeword matrix X with dimension of N_{TxT}, where N_T is the number of transmit antennas and T is the number of symbols for each block. Let a row vector x_i denote the i^{th} row of the codeword matrix X. Then, x_i will be transmitted by the i^{th} transmit antenna over the period of T symbols. In order to facilitate computationally-efficient ML detection at the receiver, the following property is required:

$$XX^H = c\left(\left|x_i^1\right|^2 + \left|x_i^2\right|^2 + \ldots\ldots\ldots + \left|x_i^T\right|^2\right) I_{N_T} = c\,\|x_i\|^2 I_{N_T} \tag{5.12}$$

Where c is a constant. The above property implies that the row vectors of the codeword matrix XX^H are orthogonal to each other, that is,

$$x_i x_j^H = \sum_{t=1}^{T} x_i^t \left(x_j^t\right)^* = 0, \quad i \neq j,\ i,j \in \{1,2,\ldots\ldots,N_T\} \tag{5.13}$$

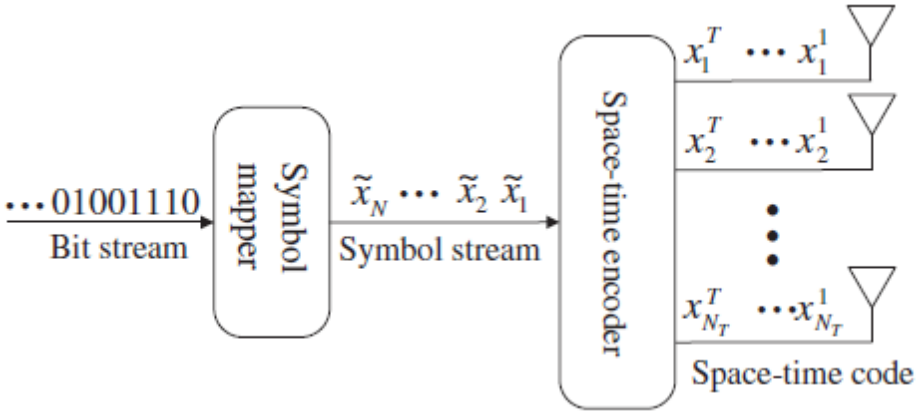

Fig 5.2 Generalised STBC[24]

5.2.2.1 Real Space-Time Block-Codes

This section provides the examples of the space-time block codes with real entries. We consider square space-time codes with the coding rate of 1 and diversity order for $N_{T=}$ 2, 4, 8.

$$X_{2,\text{real}} = \begin{bmatrix} x_1 & -x_2 \\ x_2 & x_1 \end{bmatrix}$$

$$X_{2,\text{real}} = \begin{bmatrix} x_1 & -x_2 & -x_3 & -x_4 \\ x_2 & x_1 & x_4 & -x_3 \\ x_3 & -x_4 & x_1 & x_2 \\ x_4 & x_3 & -x_2 & x_1 \end{bmatrix}$$

$$X_{3,\text{real}} = \begin{bmatrix} x_1 & -x_2 & -x_3 & -x_4 \\ x_2 & x_1 & x_4 & -x_3 \\ x_3 & -x_4 & x_1 & x_2 \end{bmatrix}$$

$$\nu = \min_{p \neq q} \text{rank} \left\{ \left(X_{3,\text{real},p} - X_{3,\text{real},q}\right)\left(X_{3,\text{real},p} - X_{3,\text{real},q}\right)^T \right\} \tag{5.14}$$

$$= \min_{p \neq q} \operatorname{rank} \left\{ \begin{bmatrix} e_1 & -e_2 & -e_3 & -e_4 \\ e_2 & e_1 & e_4 & -e_3 \\ e_3 & -e_4 & e_1 & e_2 \end{bmatrix} \begin{bmatrix} e_1 & e_2 & e_3 \\ -e_2 & e_1 & -e_4 \\ -e_3 & e_4 & e_1 \\ -e_4 & -e_3 & e_2 \end{bmatrix} \right\}$$

$$= \min_{p \neq q} \operatorname{rank} \{(|e_1|^2 + |e_2|^2 + |e_3|^2 + |e_4|^2)\mathrm{I}_3\} = 3. \qquad (5.15)$$

It is clear that $\mathrm{X}_{3,\mathrm{real}}$ achieves the maximum diversity gain of 3. The maximum diversity gain of the other real space-time code words can be shown in a similar way.

5.2.2.2 Complex Space-Time Block Code

Recall that the Alamouti code is a complex space-time block code with N_T =2, which achieves the maximum diversity order of 2 with the maximum possible coding rate [2] given as.

$$\mathrm{X}_{2,\mathrm{complex}} = \begin{bmatrix} x_1 & -x_2^* \\ x_2 & x_1^* \end{bmatrix} \qquad (5.16)$$

When N_T=3, however, it has been known that there does not exist a complex space-time code that satisfies two design goals of achieving the maximum diversity gain and the maximum coding rate at the same time. Consider the following examples for N_T=3 and N_T=4 :

$$\mathrm{X}_{3,\mathrm{complex}} = \begin{bmatrix} x_1 & -x_2 & -x_3 & -x_4 & x_1^* & -x_1^* & -x_3^* & -x_4^* \\ x_2 & x_1 & x_4 & -x_3 & x_2^* & x_1^* & x_4^* & -x_3^* \\ x_3 & -x_4 & x_1 & x_2 & x_3^* & -x_4^* & x_1^* & x_2^* \end{bmatrix}$$

$$\mathrm{X}_{4,\mathrm{complex}} = \begin{bmatrix} x_1 & -x_2 & -x_3 & -x_4 & x_1^* & -x_2^* & -x_3^* & -x_4^* \\ x_2 & x_1 & x_4 & -x_3 & x_2^* & x_1^* & x_4^* & -x_3^* \\ x_3 & -x_4 & x_1 & x_2 & x_3^* & -x_4^* & x_1^* & x_2^* \\ x_4 & x_3 & -x_2 & x_1 & x_4^* & x_3^* & -x_2^* & x_1^* \end{bmatrix}$$

If the decoding complexity at the receiver is compromised, higher coding rates can be achieved by the following codes :

$$\mathrm{X}_{3,\mathrm{complex}}^{\text{high rate}} = \begin{bmatrix} x_1 & -x_2^* & \frac{x_3^*}{\sqrt{2}} & \frac{x_3^*}{\sqrt{2}} \\ x_2 & x_1^* & \frac{x_3^*}{\sqrt{2}} & \frac{-x_3^*}{\sqrt{2}} \\ \frac{x_3}{\sqrt{2}} & \frac{x_3}{\sqrt{2}} & \frac{(-x_1 - x_1^* + x_2 - x_2^*)}{2} & \frac{(x_2 + x_2^* + x_1 - x_1^*)}{2} \end{bmatrix}$$

5.3 Decoding for Space-Time Block Codes

In this section, we consider some examples of space-time block decoding for the various code words in the previous section. The space-time block codes can be used for various numbers of receive antennas. However, only a single receive antenna is assumed in this section. Let us first consider a real space-time block code X_4,real, we express the received signals as

$$[y_1\ y_2\ y_3\ y_4] = \sqrt{\frac{E_x}{4N_0}}\,[h_1\ h_2\ h_3\ h_4]\begin{bmatrix} x_1 & -x_2 & -x_3 & -x_4 \\ x_2 & x_1 & x_4 & -x_3 \\ x_3 & -x_4 & x_1 & x_2 \\ x_4 & x_3 & -x_2 & x_1 \end{bmatrix} + [z_1\ z_2\ z_3\ z_4],$$

from which the following input-output relationship can be obtained:

$$\underbrace{\begin{bmatrix} y_1 \\ y_2 \\ y_3 \\ y_4 \end{bmatrix}}_{y_{eff}} = \sqrt{\frac{E_x}{4N_0}}\ \underbrace{\begin{bmatrix} h_1 & h_2 & h_3 & h_4 \\ h_2 & -h_1 & h_4 & -h_3 \\ h_3 & -h_4 & -h_1 & h_2 \\ h_4 & h_3 & -h_2 & -h_1 \end{bmatrix}}_{H_{eff}} \underbrace{\begin{bmatrix} x_1 \\ x_2 \\ x_3 \\ x_4 \end{bmatrix}}_{X_{eff}} + \underbrace{\begin{bmatrix} z_1 \\ z_2 \\ z_3 \\ z_4 \end{bmatrix}}_{Z_{eff}} \tag{5.17}$$

Note that the columns of the effective channel matrix H_{eff} are orthogonal to each other. Using the orthogonality of the effective channel, we can decode as

$$\tilde{y}_{eff} = H_{eff}^{T} y_{eff} \tag{5.18}$$

$$= \sqrt{\frac{E_x}{N_0 4}}\, H_{eff}^{T} H_{eff} x_{eff} + H_{eff}^{T} z_{eff}$$

$$= \sqrt{\frac{E_x}{N_0 4}} \sum_{i=1}^{4} |h_i|^2 I_4 x_{eff} + \bar{z}_{eff} \tag{5.19}$$

Using the above result, the ML signal detection is performed as

$$\hat{x}_{i,ML} = Q\left(\frac{\tilde{y}_i}{\sqrt{\frac{E_x}{4N_0}}\sum_{j=1}^{4}|h_j|^2}\right), \quad i = 1, 2, 3, 4.$$

CHAPTER 6

MATHEMATICAL ANALYSIS OF BIT ERROR RATE PERFORMANCE IN MIMO-OFDM

Let a signal x (t) is transmitted from one transmitting antenna and propagated signal fades due to reflection, refraction, dispersion, scattering and other such type of phenomenon. There are various multipath fading channel models exist. Most common fading model is Rayleigh, Rician and Nakagami-m fading channel. Rayleigh channel is basically the complex Gaussian noise. Rayleigh channel is generated when incoming signal is received from large number of scatters. If there is one or more numbers of dominant path (basically LOS) [24] exist between transmitter and receiver, the channel becomes Rician. Another fading channel is Nakagami-m channel. Here, we derive the expression in Rayleigh fading channel, whose gain is denoted by h (t), and AWGN is denoted by n (t).

6.1 Probability of Error for $N_T = 1$, $N_R = 1$ in Rayleigh Fading Channel

The received signal y(t) is expressed as (assume delay spread is less than time period of symbol) :

$$y(t) = h(t)\, x(t) + n(t)$$

$$y = hx + n$$

$$y = z + n \qquad (z = hx)$$

Let $z_1 = hx$

Probability density function of h (t) $(\mathrm{PDF}) = f_h(h)$

$$\mathrm{PDF\,of}\ x(t) = f_x(x)$$

Probability density function of z = hx is given as:-

$$f_z(z) = \int_{-\infty}^{\infty} \frac{1}{|x|} f_{xh}\left(x, \frac{z}{x}\right) dx$$

$$= \int_{-\infty}^{\infty} \frac{1}{|x|} f_x(x) f_n\left(\frac{z}{n}\right) dx \qquad (6.1)$$

Let the phase estimation is done at the receiver side, the magnitude of complex channel gain $|h|e^{jwt}$ follows Rayleigh PDF.

PDF of |h| is given as

$$f_n(r) = \frac{r}{\sigma^2} e^{-\frac{r^2}{2\sigma^2}}$$

where σ is the variance.

$$f_z(z) = \int_{-\infty}^{\infty} \frac{1}{|x|} \delta\left(x - \sqrt{E_b}\right) \times \frac{\left(\frac{z}{x}\right)}{\sigma^2} e^{-\left(\frac{z}{n}\right)^2 \times \frac{1}{2\sigma^2}} dx$$

$$= \frac{1}{\sqrt{E_b}} \times \frac{Z}{\sqrt{E_b}\sigma^2} e^{-\frac{z^2}{2\sigma^2} \times \frac{1}{E_b}} \quad (6.2)$$

where E_b is the bit energy.

$$f_z(z) = \frac{z}{E_b \sigma^2} e^{-\frac{z^2}{2\sigma^2 . E_b}} \quad (6.3)$$

$$y = z + n$$

z & n are independent. PDF of sum of z and n is the convolution of $f_z(z)$ and $f_n(n)$, then

PDF of received signal y is $f_y(y) = \int_{-\infty}^{\infty} f_z(z) f_n(y - z) dz$

where $x = \sqrt{E_b}, z \in \{0, \infty\}$

$$f_y(y) = \int_0^{\infty} \frac{1}{E_b} \frac{z}{\sigma^2} e^{-\frac{z^2}{2\sigma^2 . E_b} \times \frac{1}{\sqrt{2n\sigma^2}}} e^{-\frac{(y-2)^2}{2\sigma^2}} dz \quad (6.4)$$

$$f_y(y) = \frac{1}{\sqrt{2\pi}E_b} \int_0^{\infty} z.e^{-\left[\frac{Z^2 + (y-z)^2 E_b}{2E_b}\right]} dz$$

In case of orthogonal signals, correlater is used as the receiver side to separate them. Let there are N orthogonal signal $y_1, y_2, y_3 \ldots\ldots\ldots\ldots y_n$.

The equation of output at the correlater is given below :

y signal received, $y = |h|\sqrt{E_b} + n_1$

n_2

|

|

n_n

Where $n = 1, 2, 3 \_ \_ \_ \_ \_ \_ \_ \_ \_ N$

Joint PDF of $y_1, n_2, n_3 ----n_n$

$$f_{y_1 n_1 \ldots\ldots n_n} = f_y(y_1) f(n_2) \ldots\ldots\ldots f(n_n)$$

PDF of $Y_{1,}$ which has maximum SNR i.e.

$$f_{Y1}(Y_1) = \int_{-\infty}^{y_1}\int_{-\infty}^{y_1}\int_{-\infty}^{y_1} f_y(y) f_n(n_2) \ldots . f_n(n_n)\ dn_2 dn_3 \ldots dn_n$$

$$f_{Y1}(Y_1) = f_y(y_1)\left[\int_{-\infty}^{y1} f_n(n)\,dn\right]^{N-1} \tag{6.5}$$

Equation (6.5) gives the PDF of orthogonal signal. Hence, probability of error in case of BPSK (using ML dection) , is given by the following equation :

$$P_e = \int_{-\infty}^{0} f_{Y1}(Y_1)\,dY_1 \tag{6.6}$$

Equation (6.6) can be extend for No. of Transmitting N_T = 4, No. of receiving antenna N_R = 4.

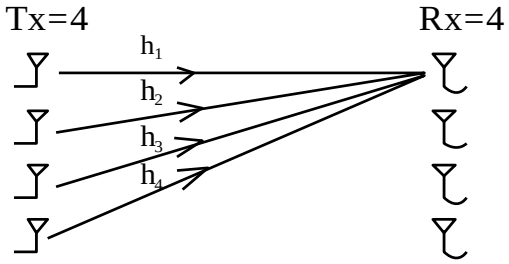

Fig 6.1 *MIMO System for N_T = 4, N_R = 4.*

Received signal at one of the receiving antennas is given by

$$Y = h_1x_1 + h_2x_2 + h_3x_3 + h_4x_4 + n$$

Let $y = h_1 x_1 + n$

$z_2 = h_2 x_2$

$z_3 = h_3 x_3$

$z_4 = h_4 x_4$

Their joint PDF

$$f_{yz_2z_3z_4} = f(y)f(z_2)f(z_3)f(z_4)$$

$$f_{yz_2z_3}(Y) = f(y)f(z_2)f(z_3)f(Y - y - z_2 - z_3)$$

$$f_y(Y) = \int_{-\infty}^{\infty}\int_{-\infty}^{\infty}\int_{-\infty}^{\infty} f_{y_1}(y) f_z(z_2) f_z(z_3) f_z(Y - y - z_2 - z_3)\ dy\, dz_2 dz_3$$

$$Pe = \int_{-\infty}^{o} f_y(Y)\, dy \qquad (6.7)$$

Hence equation (6.7) gives the probability of error for $T_x = 4,\ T_R = 1$.

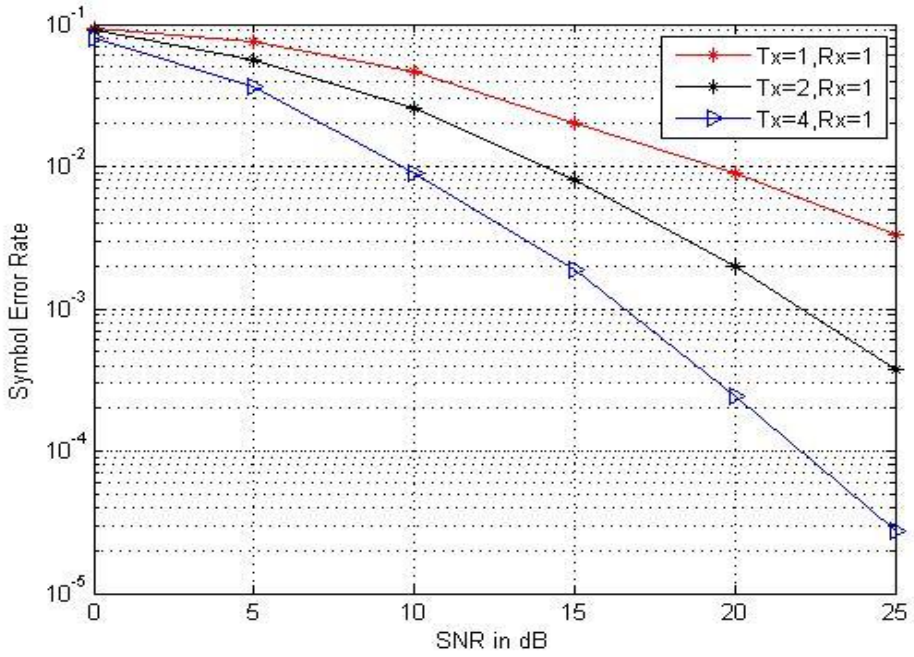

Fig 6.2 *SER performance in OFDM system with different diversity order*

Fig. 6.2 shows that the SER decreases with increase in the number of transmitting antennas. The SER performance is investigated in 16-QAM modulation scheme. SER(10^{-2}) is achieved at SNR=10 dB, if number of transmit antennas is four, but same performance is obtained at 19 dB (SNR) when one transmit and one receiving antenna is used. Hence, 9 dB is saved (in case of four transmit antennas) , but the complexity and cost of the system increases.

Number of T_x = 4

Number of T_R = 4

Here selection diversity is used, select the one from $Y_1, Y_2, Y_3 \& Y_4$; which has maximum SNR

i.e. $Y_1 > Y_2, Y_3, Y_4$

Assume correct signal is received at antenna 1.

Joint PDF of Y_1, Y_2, Y_3, Y_4

$$f_{Y_1Y_2Y_3Y_4}(Y_1, Y_2, Y_3, Y_4) = f(Y_1) f(Y_2) f(Y_3) f(Y_4)$$

$$P_e = \int_{-\infty}^{0} \int_{-\infty}^{Y_1} \int_{-\infty}^{Y_1} \int_{-\infty}^{Y_1} f(Y_2) f(Y_3) f(Y_4) f(Y_1) \; dY_2 \, dY_3 dY_4 \, dY_1$$

$$P_e = \int_{-\infty}^{0} \left[\int_{-\infty}^{\gamma_1} f_Y(Y) dY \right]^3 f_{Y_1}(Y_1) dY_1$$

6.2 Probability of Error For Tx=1, Rx=1 when Zero-Forcing Equalization is used

$$y = hx + n$$

Then estimate value of received signal is

$$\hat{y} = x + \frac{x}{h}$$

$$f_x(x) = \delta\left(x - \sqrt{E_b}\right)$$

$$f(h) = \frac{r}{\sigma^2} e^{-\frac{r^2}{2\sigma^2}}$$

$$f_n(n) = \frac{1}{\sqrt{2\pi}} e^{-\frac{\pi^2}{2}} \qquad \text{Let } Z = \frac{x}{h}$$

$$f\left(\frac{x}{h}\right) = \int_{-\infty}^{\infty} |n| f_{nh}(nz, h)\, dh$$

$$= \int_{-\infty}^{\infty} |n| f_n(n_z) f_h(h)\, dh$$

$$f_z(Z) = \frac{1}{\pi(1+z^2)} \qquad \text{Re}\left[z^2\right] > -1$$

$$f_y = \frac{1}{\pi\left(1 + E_b - 2\sqrt{E_b} y + (y)^2\right)}$$

$$P_e = \int_{-\infty}^{0} \frac{1}{\pi\left(1 + E_b - 2\sqrt{E_b} y, + y^2\right)} dy$$

$$P_e = \frac{\pi - 2\tan^{-1}\left[\sqrt{E_b}\right]}{2\pi} \tag{6.8}$$

6.3 Probability of Error in Flat Rayleigh Fading Channel

Wireless channels with relatively small bandwidth are typically characterized as the Rayleigh-fading channel. The Rayleigh fading leads to a significant degradation in BEP performance compared to the Gaussian channel, since the Rayleigh fading decreases the SNR. In the Gaussian channel, the BEP decreases exponentially with the SNR, while in the Rayleigh fading channel, it decreases linearly with the average SNR. Diversity, spread spectrum and OFDM are the three techniques to overcome fading.

The BEP of Rayleigh fading can be derived as

$$P_b^{Rayleigh} = \int_0^{\infty} P_b\left(\overline{\gamma_b} \mid r\right) P_r(r)\, dr \tag{6.9}$$

where $P_r(r)$ is the Rayleigh PDF and $\overline{\gamma_b} = \frac{\overline{E_b}}{N_0} = \frac{2\sigma^2 E_b}{N_0}$ is the mean bit SNR, σ being a

parameter of the Rayleigh PDF.

The SEP for Rayleigh fading can be derived from (6.9). First, at each instant, the amplitude of the received signal, r, satisfies the Rayleigh distribution. Define the received power as $P_{inst} = r^2,$ and then the mean power is $\bar{P} = 2\sigma^2$. Since $dP_{inst} = 2rdr,$ the PDF of the received power $p_{inst}(P_{inst})$ can be derived. By scaling P_{inst} by $1/N_0$, the PDF of the symbol SNR γ_s, $p_{\gamma_s}(\gamma),$ is derived as

$$p_{\gamma_s}(\gamma) = \frac{1}{\bar{\gamma}_s} e^{-\frac{\gamma}{\gamma_s},} \tag{6.10}$$

Where $\bar{\gamma}_s = \frac{\overline{E_s}}{N_0}$ is the mean symbol SNR. The SEP of the Rayleigh fading channel is finally obtained by averaging over the distribution of the symbol SNR

$$p_s^{Rayleigh} = \int_0^{\infty} p_{\gamma_s}(\gamma) P_s(\gamma) d\gamma, \tag{6.11}$$

where $P_s(\gamma)$ is the SEP in the AWGN channel. This procedure is also valid for Ricean fading and other amplitude distributions.

In the AWGN channel, many coherent demodulation methods have an approximate or exact value for P_s of the form

$$P_s(\gamma_b) \approx c_1 Q\left(\sqrt{c_2 \gamma_b}\right) \tag{6.12}$$

Another general form for P_s in the AWGN channel is

$$P_s(\gamma_b) \approx c_1 e^{-c_2 \gamma_b,} \tag{6.13}$$

where c_1 *and* c_2 are constants.

Corresponding to (6.12), the SEP in the Rayleigh fading channel can be derived by substituting (6.12) in (6.11).

$$P_s^{Rayleigh} = \frac{c_1}{2}\left(1 - \sqrt{\frac{c_2 \bar{\gamma}_b}{2 + c_2 \bar{\gamma} b}}\right) \tag{6.14}$$

At high γ_b, $p_s^{Rayleigh} \approx \frac{c_1}{2_{c_2}\,\bar{\gamma}_b}$

Also, corresponding to (6.13), the SEP in the Rayleigh fading channel can be obtained by substituting (6.13) in (6.11).

$$P_s^{Rayleigh} = \frac{c_1}{1 + c_2 \overline{\gamma}_b} \tag{6.15}$$

Closed – form results for MPSK, DMPSK, and MQAM for MPSK ,

A closed- form expression for the flat Rayleight fading channel is given by

$$P_s^{Rayleigh} = \frac{M-1}{M} - \alpha\left[\frac{1}{2} + \frac{1}{\pi}\tan^{-1}\left(\alpha\cot - \frac{\pi}{M}\right)\right] \text{(MPSK, Rayleigh)} \tag{6.16}$$

For DMPSK, closed-form SEP formula for fast Rayleigh channels is derived as

$$P_s = \frac{M-1}{M} + \frac{|\rho_z|\tan(\pi/M)}{\xi(\rho_z)}\left[\frac{1}{\pi}\arctan\left(\frac{\xi(\rho_z)}{|\rho_z|}\right) - 1\right] \text{ (DMPSK, fast Rayleigh channel)} \tag{6.17}$$

where

$$\rho_z = \frac{\overline{\gamma}}{1+\overline{\gamma}}\rho\alpha,$$

$$\xi(\rho_z) = \sqrt{1 - |\rho_z|^2 + \tan^2\left(\frac{\pi}{M}\right)}$$

ρ_α denotes the correlation between α_k and $\alpha_k - 1, \alpha_k$ being the received signal phase difference. When M = 2, it reduces to

$$P_s = \frac{1}{2}\left(1 - \frac{\overline{\gamma}}{1+\overline{\gamma}}|\rho_\alpha|\right)$$

As $\gamma \to \infty, |\rho_z| \to |\rho_\alpha|, P_s$ reveals the presence of an error floor for DMPSK on fast fading channels. On low fading channels, $\rho_\alpha = 1$, we have

$$P_s = \frac{M-1}{M} - \frac{1}{\pi}\sqrt{\frac{\overline{\gamma}^2\sin^2\left(\frac{\pi}{M}\right)}{1 + 2\overline{\gamma} + \overline{\gamma}^2\sin^2\left(\frac{\pi}{M}\right)}} \times \left[\pi - \arccos\left(\frac{\overline{\gamma}}{1+\overline{\gamma}}\cos\left(\frac{\pi}{M}\right)\right)\right] \tag{6.18}$$

6.4 Probability of Error in Flat Ricean Fading Channel

The SEP for the Ricean fading channel can also be computed from (6.11), but $p_{\gamma_s}(\gamma)$ for Ricean fading is used. Closed-form BEP expressions are derived for optimum DBPSK and non-coherent BFSK [30]

$$P_b = \frac{K_r + 1}{2\left(K_r + 1 + \overline{\gamma}_b\right)} e^{-\frac{K_r \overline{\gamma} b}{K_r + 1 + \overline{\gamma} b}} \qquad \text{(optimum DBPSK),}$$

$$P_b = \frac{K_r + 1}{2\left(K_r + 1\right) + \overline{\gamma}_b} e^{-\frac{K_r \overline{\gamma}_b}{2(k_r + 1) + \overline{\gamma}_b}} \qquad \text{(non-coherent BFSK),}$$

For other modulation schemes, numerical integration has to be used for calculating the BEP performance in the Rician channel.

The BEP performance in the Ricean fading channel lies between that in the AWGN and Rayleigh fading channels. For $K_r \to 1$, it reduces to Rayleigh fading, while for $K_r \to \infty$, we obtain the AWGN channel.

Alternative Form of the Q-Function

The Q-function is most fundamental for BEP calculation. Its integration limit that runs to infinity makes its calculation very difficult. Recently, the following representation of the Q-function has been introduced and it makes the computation much more efficient.

$$Q(x) = \frac{1}{\pi} \int_0^{\pi/2} e^{-\frac{x^2}{2\sin^2\theta}} d\theta, \quad x > 0. \tag{6.20}$$

By using this new Q-function, one can very easily calculate the BEP or SEP related to the Q-function. The alternative Q-function makes the derivation of closed-form BEP or SEP, or its numerical calculation much easier.

The SEP in fading channels can be written in generic form :

$$P_s(\gamma) = \int_{\theta_1}^{\theta_2} f_1(\theta) e^{-\gamma f_2(\theta))} d\theta.$$

The SEPs of MPSK, MASK, and M-QAM, given in terms of Q-function can be calculated by using the alternative Q-function representation

$$P_s = a\int_0^b e^{-\frac{c\gamma s}{\sin^2\theta}} d\theta,$$

where

$$a = \frac{2}{\pi}\frac{M-1}{M}, \qquad b = \frac{\pi}{2}, \qquad c = \frac{3}{M^2-1} \quad (\text{MASK}),$$

$$a = \frac{4}{\pi}\frac{\sqrt{M}-1}{\sqrt{M}}, \qquad b = \frac{\pi}{2}, \qquad c = \frac{3}{2(M-1)} \quad (\text{MQAM}),$$

$$a = \frac{1}{\pi}, \qquad b = \pi\frac{M-1}{M}, \quad c = \sin^2(\pi/M) \quad (\text{MPSK}).$$

6.5 Error Probability using Moment- Generating Functions

The average SEP can be expressed as

$$\overline{P_s} = \int_{\theta_1}^{\theta_2} f_1(\theta) M_\gamma\left(-f_2(\theta)\right) d\theta,$$

where the moment-generating function $M_\gamma(s)$ is the Laplace transform of $p_\gamma(\gamma)$, that is, $M_\gamma = \int_0^\infty p_\gamma(\gamma) e^{sy} d\gamma.$

For the Rayleigh distribution

$$M_\gamma(s) = \frac{1}{1-s\overline{\gamma}}$$

For Rice distribution

$$M_\gamma(s) = \frac{1+K_r}{1+K_r - s\overline{\gamma}} e^{\frac{K_r s\overline{\gamma}}{1+K_r - s\overline{\gamma}}}$$

The average (ergodic) error probability in fading for modulation with P_s in the AWGN channel, which is given by (6.12), can be calculated by

$$\bar{P}_s = \frac{\alpha_M}{\pi}\int_0^{\pi/2} M_{\gamma_s}\left(\frac{-\beta_M}{2\sin^2\theta}\right)d\theta \tag{6.21}$$

For the Rayleigh distribution, the exact average probability of error for M-ary linear modulation in fading is given by

$$\bar{P}_s = a\int_0^b M_{\gamma_s}\left(\frac{-c}{\sin^2\theta}\right)d\theta.$$

For statistically independent diversity branches, we have

$$\bar{P}_s = a\int_0^b \prod_{l=1}^{N_r} M_{\gamma_s,l}\left(\frac{-c}{\sin^2\theta}\right)d\theta = a\int_0^b \left[M_{\gamma_s}\left(\frac{-c}{\sin^2\theta}\right)\right]^{N_r} d\theta \tag{6.22}$$

where N_r is the diversity order.

The ergodic error probability in the Rayleigh fading channel can thus be obtained as

$$\bar{P}_s = a\int_0^b \left(\frac{N_r \sin^2\theta}{N_r \sin^2\theta + c\gamma s}\right)^{N_r} d\theta$$

Error Probabilities due to Delay Spread and Frequency Dispersion

Frequency-selective fading leads to ISI, while Doppler gives rise to spectrum broadening which leads to ACI. Doppler spread has a significant influence on the BEP performance of modulation techniques that use differential detection. BEPs due to delay spread (frequency selective fading) or frequency dispersion (Doppler spread) can not be reduced by increasing the transmit power, thus they are called error floors. For low data rate systems such as sensor networks or paging, the Doppler shift can lead to an error floor of an order of up to 10^{-2}. Generally, for high data rate wireless communications such as mobile communications and wireless LAN, error due to frequency dispersion is of the order of up to 10^{-4}, which is very small compared with that arising from noise

Error Probability Due To Frequency Dispersion

For DPSK in fast Ricean fading, where the channel decorrelates over a bit period, the BEP is given by

$$\bar{P}_b = \frac{1}{2}\left(\frac{1+K_r+\bar{\gamma}_b(1-\rho_c)}{1+K_r+\bar{\gamma}_b}\right)e^{-\frac{K_r\bar{\gamma}_b}{1+K_r+\bar{\gamma}_b}}$$

where K_r is the fading parameter of Ricean distribution, and ρ_c is the chanel correlation coefficient after a bit period T_b. For the uniform scattering Doppler spectrum model, from Section 3,3.1, the Doppler power spectrum is

$$S(f) = \frac{P_0}{\pi\sqrt{v_{\max}^2 - f^2}}, |f| < v_{\max}$$

then $\rho_c = \phi_c(T)/\phi_c(0) = J_0(2\pi v_{\max} T)$. For the rectangular Doppler power spectrum model, $S(f) = P_0/2v_{\max}, |f| < v_{\max}$, then $\rho_c = \sin c(2v_{\max}T)$.

For Rayleigh fading, $K_r = 0$, we have

$$\bar{P}_b = \frac{1}{2}\left(\frac{1+\bar{\gamma}_b(1-\rho_c)}{1+\bar{\gamma}_b}\right)$$

The irreducible error floor for DPSK is obtained by limiting $\gamma_b \to \infty in$

$$\bar{P}_{b,\,floor} = \frac{(1-\rho_c)e^{-K_r}}{2}$$

The irreducible bit error floor for DQPSK is fast Rician fading is derived as

$$\bar{P}_{b,\,floor} = \frac{1}{2}\left(1-\sqrt{\frac{\left(\rho_c/\sqrt{2}\right)^2}{1-\left(\rho_c/\sqrt{2}\right)^2}}\right)e^{-\frac{(\sqrt{2}-1)K_r}{\sqrt{2}-\rho c}}$$

where ρ_c is the chanel correlation coefficient after a symbol time T.

For the uniform scattering model and Rayleigh fading, the irreducible error for DPSK is obtained as

$$\bar{P}_{b,\,floor} = \frac{1}{2}\left[1-J_0(2\pi v_{\max}T_b)\right] \approx 0.5(\pi v_{\max}T_b)^2$$

For small $v_{\max}T_b$, the BEP is generally given by

$$\bar{P}_{b,\,\text{Doppler}} = K(v_{\max}T_b)^2$$

Here K is a constant, Note that the error floor decreases as the data rate R = $1/T_b$ increases. For MSK, K = $\pi^2/2$.

Error Probability due to Delay Dispersion

For delay dispersion, ISI influences as significant percentage of each symbol. For Rayleigh fading, when the maximum excess delay of the channel is much smaller than the symbol duration, the error floor due to delay dispersion is given by

$$\bar{P}_{b.\,floor} = K\left(\frac{\sigma_\tau}{T_b}\right)^2$$

where σ_τ is the rms delay spread of the channel and K is a constant, which depends on the system implementation. For differentially detected MSK, K= 4/9 , the error floor due to delay dispersion is typically more significant than that due to frequency dispersion for high data rate.

Error Probability in Fading Channels with Diversity Reception

The average SEP in a flat-fading channel is derived by the distribution of the SNR

$$\bar{P}_s = \int_0^\infty p_\gamma(\gamma) P_s(\gamma)\, d\gamma$$

For BPSK signals in the Rayleigh fading channel, the SEP for N_r diversity branches with MRC is given by

$$\bar{P}_s = \left(\frac{1-\mu}{2}\right)^{N_r} \sum_{k=0}^{N_r-1} \binom{N_r-1+k}{k} \left(\frac{1+\mu}{2}\right)^k$$

where

$$\mu = \sqrt{\frac{\bar{\gamma}_s}{1+\bar{\gamma}_s}} \qquad (6.23)$$

For large $\bar{\gamma}_s$, the SEP is well approximated by

$$P_s = \left(\frac{1}{4\bar{\gamma}_s}\right)^{Nr} \binom{2N_r-1}{N_r}$$

Thus, the BEP decreases with the N_r th power of the average SNR. For a MIMO system of N_t transmitting antennas and N_r receiving antennas, there are altogether N_tN_r diversity branches, and thus N_r in the above equation is replaced by N_tN_r.

For the AWGN channel, consider the error probability of the form

$$P_s = \frac{1}{2}e^{-\alpha\gamma s}$$

where $\alpha = 0.5$ for non-coherent FSK and $\alpha = 1$ for differential coherent PSK. For N_r diversity branches, we have the error probability for both cases

$$P_b = \frac{1}{2}\prod_{k=1}^{N_r}\frac{1}{1+\alpha\bar{\gamma}_{s,k}} \text{(MRC)},$$

$$P_b = \frac{1}{2}\frac{N_r!}{\prod_{k=1}^{Nr}\left(k+\alpha\bar{\gamma}_s\right)} \text{ (Selection diversity)}$$

$$P_b = \frac{\left(\frac{N_r}{2}\right)^{N_r}\sqrt{\pi}}{2\left(N_r-\frac{1}{2}\right)}\prod_{k=1}^{N_r}\frac{1}{1+\alpha\bar{\gamma}_{s,k}} \text{ (EGC)}$$

For coherent FSK and coherent PSK in the AWGN channel where $\alpha = 0.5$ for coherent FSK and $\alpha = 1$ for coherent PSK. For N_r diversity branches the average error probability is derived by taking $p(\gamma)$. There is no convenient closed-form solution in case of all branches being equal in strength $\bar{\gamma}_s$, we have

$$P_s = \frac{1}{2\sqrt{\pi}}\frac{1}{\left(\alpha\bar{\gamma}_s\right)^{N_r}}\frac{\left(N_r-\frac{1}{2}\right)!}{N_r!} \tag{6.24}$$

By using the moment-generating function and the trigonometric form of the Q-function, the average SEP of an MRC diversity system can be derived as

$$\bar{P}_s = \int_{\theta_1}^{\theta_2} d\theta\, f_1(\theta)\left[M_{\gamma_s}\left(-f_2(\theta)\right)\right]^{N_r}$$

For BPSK in Rayleigh fading, the SEP is alternatively given by

$$\bar{P}_s = \frac{1}{\pi}\int_0^{\pi/2}\left(\frac{\sin^2\theta}{\sin^2\theta+\bar{\gamma}_s}\right)^{N_r} d\theta$$

Diversity can also improve the SEP performance of frequency-selective and time-selective fading channels. Generally, the SEP with diversity is approximately the N_rth power of the BEP without diversity.

CHAPTER 7

QUASI-ORTHOGONAL SPACE-TIME BLOCK-CODED OFDM WIRELESS MOBILE COMMUNICATION SYSTEMS USING ARRAY-PROCESSING APPROACH

To overcome the disadvantages of OSTBC, quasi-orthogonal space–time block coding (QO-STBC) was proposed [2] that offers a higher data rate and partial diversity gain. A novel decoding approach for QO-STBC OFDM is introduced, and it works based on an array-processing technique. The received QO-STBC OFDM symbol array is decomposed by null spaces[20] of the split-up channel matrices, followed by a parallel decoding unit, as an effort to reduce the computational complexity and latency induced by the decoding process. The performance of the proposed system is evaluated over frequency-selective channel by both analysis and computer simulations to show the effectiveness of the scheme. Maximum likelihood (ML) decoding in QO-STBC [27] works with maximum- pairs of transmitted symbols, leading to an increase in decoding complexity with modulation level 2M. This subsequently increases transmission delay when a high-level modulation scheme or multiple antennas are employed. Some new decoding methods were proposed to reduce the computational complexity. A QO-STBC with minimum decoding complexity (MDC-QO-STBC) was proposed[28] by introducing a new coding scheme. However, they either are still too complex, if compared with Alamouti coding or require more complex signal processing at the transmitter end. This is particularly true for their applications in QO-STBC OFDM systems, in which space–time coding is implemented based on vectors instead of symbols. To further reduce the complexity of the decoding scheme, we propose a new decoding approach that combines decoding with array processing[20]. By making use of the null space of split-up MIMO channel matrices, a received symbol is decomposed into several independent parts, which are then decoded in a parallel way. The complexity of this approach was evaluated, and it increases with 2M, which is considerably lower than that of all traditional schemes. Unfortunately, in a QO-STBC OFDM system, the decoding method proposed can not directly be utilized, as coding here is based on OFDM symbols, which are vectors rather than scalars. Each element of the channel matrix turns out to be a vector,

making it impossible to calculate their null spaces. To solve this problem, we decode the OFDM symbols using a sample-by-sample approach.

7.1 System Model

The symbol matrix X where vector *n* is the system complex noise, modulated as independent identically distributed (i.i.d.) Gaussian random variables, which have zero mean and unit variance *E[n(n*)]=I.* Without loss of generality, we focus on a multiple-input and multiple-output (MIMO) system, which has four antennas at the transmitter and four antennas at the receiver. The source bits are modulated with M-QAM. Then, the serial modulated symbols are transferred and stacked as a symbol vector $x = [x_1, x_2, x_3, x_4]$. This vector afterwards will be transformed into a transmission matrix X by a QO-STBC encoder. The n^{th} row elements of X are transmitted by the n^{th} transmitting antenna. The t^{th} column elements are transmitted at time slot t. We assume that the MIMO channel is a Rayleigh fading channel, denoted by *H,* the element *h(m,n)* of *H* represents the path gain between the n^{th} transmit and m^{th} receiver antenna. Then, the received signal vector r can be written as

$$r = HX + n \qquad (7.1)$$

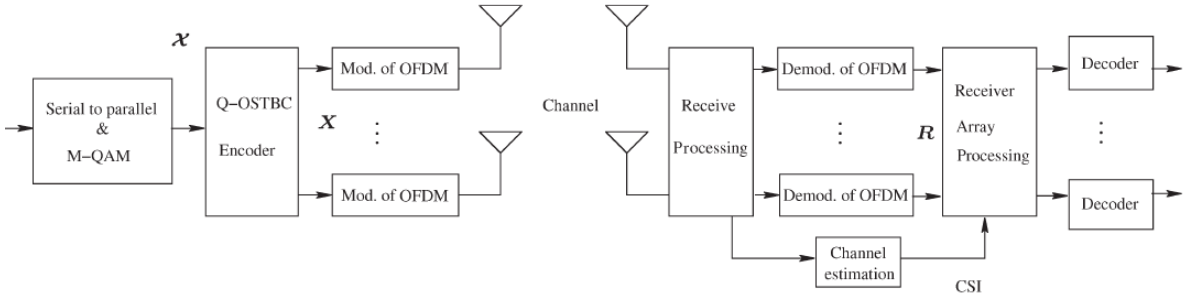

Fig. 7.1 Block diagram of MIMO-OFDM wireless communication system[20].

7.1.1 Frequency-Selective Channel Model

The channel model chosen in our study is a one-ring-based geometric model[32]. In this model, the antenna element spacing at the BS and the MS are designated by δ_{BS} and δ_{MS}, respectively, and the angles between the antenna array and the line connecting the BS and the

MS are denoted by α_{BS} and α_{MS}. Without loss of generality, it is assumed that both of them are equal to 90 degree. Φ is defined as the angle of arrival (AOA) of the n^{th} incoming wave seen at the MS, and the corresponding angle of departure is denoted by ϕ_n^{MS} . α_v is the angle of motion, which denotes the movement direction of the MS. Assume that there are L paths and that each path has N_L scatters allocated on a ring around an MS of radius R. The distance between the BS and the MS is assumed to be fairly larger than the radius of the ring around the MS. If we define c_ℓ and τ_ℓ as the attenuation factor and the time delay of path ℓ, respectively, the time-variant complex channel gain describing the link from the *q*th transmit antenna to the *p*th receive antenna can be expressed as

$$g_{pq}(\tau,t) = \sum_{\ell=1}^{\mathcal{L}} \frac{c_\ell}{\sqrt{\mathcal{N}_\ell}} \sum_{n=1}^{\mathcal{N}_\ell} a_{n,q,} e^{b_{n,p,\ell.}} \; exp\left\{j\left(2\pi f_{n,\ell} t + \theta_{n,\ell}\right)\right\} \delta(\tau - T_\ell) \tag{7.2}$$

where

$$a_{n,q,\ell} = e^{j\pi(M_{BS}-2q+1)\frac{\delta_{BS}}{\lambda}\left[cos(\alpha_{BS})+\phi_{max}^{BS} \; sin(\alpha_{BS})\sin(\phi_n^{MS})\right]} \tag{7.3}$$

$$b_{n,q,\ell} = e^{j\pi(M_{MS}-2p+1)\frac{\delta_{MS}}{\lambda}\cos(\phi_n^{MS}-\alpha_{MS})} \tag{7.4}$$

$$f_{n,\ell} = f_{max} \; cos(\phi_n^{MS} - \alpha_v) \tag{7.5}$$

for $p \in \{1, 2, \ldots, M_{MS}\}$ and $q \in \{1, 2, \ldots, M_{BS}\}$. λ is the carrier wavelength, and f_{max} represents the maximum Doppler frequency. The AOA ϕ_n^{MS} and the phases θn are constants, each obeying a uniform distribution over [0, 2π). Taking the Fourier transform of $g_{pq}(\tau, t)$ with respect to τ, we get

$$h_{pq}(f,t) = \sum_{\ell=1}^{\mathcal{L}} \frac{c_\ell}{\sqrt{\mathcal{N}_\ell}} \sum_{n=1}^{\mathcal{N}_\ell} a_{n,q,\ell} \; b_{n,p,\ell} e^{j\left[2\pi\left(f_{n,\ell} t - T_{\ell f}\right) + \theta_{n,\ell}\right]} \tag{7.6}$$

channel matrix:

$$h(f,t) = \begin{bmatrix} h_{11}(f,t) & h_{12}(f,t) & \cdots & h_{1M_{BS}}(f,t) \\ h_{21}(f,t) & h_{22}(f,t) & \cdots & h_{2M_{BS}}(f,t) \\ \vdots & \vdots & \ddots & \vdots \\ h_{M_{MS}1}(f,t) & h_{M_{MS}2}(f,t) & \cdots & h_{M_{MS}M_{BS}}(f,t) \end{bmatrix} \tag{7.7}$$

in which $\boldsymbol{h}pq(\boldsymbol{f}, t)$ is a vector with its variable $\boldsymbol{f} = [f_0, f_1, \ldots, f_{N-1}]$ defined as

$$h_{pq}(f,t) = \left[H_{pq}(f_0,t) H_{pq}(f_1,t), \ldots\ldots, H_{pq}(f_{N-1},t)\right] \tag{7.8}$$

$$\mathcal{P} \in \{1,2,\ldots.,M_{MS}\}, \qquad q \in \{1,2,\ldots.,M_{BS}\}.$$

At the receiver, after OFDM demodulation, the GIs are discarded. The *k*th signal vector received at the *p*th antenna at time slot *m* is given by

$$r_p\,(m+k) = \sum_{q=1}^{M_{BS}} X_{p,k}{}^{diag\,[h_{pq}\,(f,t)]} + n_p(m), \quad \in \mathbb{C}^{1\,x\,N} \tag{7.9}$$

where $k \in \{1, 2, \ldots, K\}$, and K is the number of data blocks transmitted in one time slot. The function diag(·) is to calculate a diagonal matrix. $n_p(m)$ represents the noise vector, which is defined as

$$n_p(m) = \left[n_{p,0}(m), n_{p,1}(m), \ldots\ldots, n_{p,N-1}(m)\right]. \tag{7.10}$$

7.1.2 Decoding of QO-STBC OFDM

It is assumed that instantaneous channel state information (CSI) is always available at the receiver, since it is easy to get the real channel state by employing one channel estimation approach. The decoder chooses the decision symbol *x* from the transmission constellation M so that the decision metric can be minimized[34].

$$\hat{x} = arg_{\,x\in M} \min\|r - Hx\|^2 \tag{7.11}$$

X_{12} is transmitted from the 1st and 2nd antennas and X_{34} is transmitted from the 3rd and 4th antennas at the first time slot. Then, in the next two slots their transformed versions are transmitted, separately. Thus, if we divide the transmitted signals into two parts which will be transmitted by antenna group 1 including the 1st and 2nd antennas and group 2, including the 3rd and 4th antennas. Then the linear decoding scheme can be employed. In this way, the decoding computational load can be considerably deduced. After the division, the MIMO channel H can be rewritten as $H = [H_1, H_2]$.

At the mobile station, the received signal is

$$R_n(m) = H\left(f_{n,}t\right)X_n(m) + N_n(m) \tag{7.12}$$

Where

$$X\,(m) = \begin{bmatrix} x(m) & -x(m+1)^* & -x(m+2)^* & x(m+3) \\ x(m+1) & x(m)^* & -x(m+3)^* & -x(m+2) \\ x(m+2) & -x(m+3)^* & x(m)^* & -x(m+1) \\ x(m+3) & x(m+2)^* & x(m+1)^* & x(m) \end{bmatrix}$$

$$R(m) = \begin{bmatrix} r_1(m) & r_1(m+1) & \cdots & r_1(m+k-1) \\ r_2(m) & r_2(m+1) & \cdots & r_2(m+k-1) \\ \vdots & \vdots & \vdots & \vdots \\ r_{M_{MS}}(m) & r_{M_{MS}}(m+1) & \cdots & r_{M_{MS}}(m+k-1) \end{bmatrix}$$

$$H(f,t) = \begin{bmatrix} \widehat{H}_{11}(f,t) & \widehat{H}_{12}(f,t) & \cdots & \widehat{H}_{1M_{BS}}(f,t) \\ \widehat{H}_{21}(f,t) & \widehat{H}_{22}(f,t) & \cdots & \widehat{H}_{2M_{BS}}(f,t) \\ \vdots & \vdots & \ddots & \vdots \\ \widehat{H}_{M_{MS}1}(f,t) & \widehat{H}_{M_{MS}2}(f,t) & \cdots & \widehat{H}_{M_{MS}M_{BS}}(f,t) \end{bmatrix}$$

$$R_n(m) = \begin{bmatrix} r_{1,n}(m) & r_{1,n}(m+1) & \cdots & r_{1,n}(m+K-1) \\ r_{2,n}(m) & r_{2,n}(m+1) & \cdots & r_{2,n}(m+K-1) \\ \vdots & \vdots & \vdots & \vdots \\ r_{M_{MS},n}(m) & r_{M_{MS},n}(m+1) & \cdots & r_{M_{MS},n}(m+K-1) \end{bmatrix}$$

$$X_n = \begin{bmatrix} x_n(m) & -x_n(m+1)^* & -x_n(m+2)^* & x_n(m+3) \\ x_n(m+1) & x_n(m)^* & -x_n(m+3)^* & -x_n(m+2) \\ x_n(m+2) & -x_n(m+3)^* & x_n(m)^* & -x_n(m+1) \\ x_n(m+3) & x_n(m+2)^* & x_n(m+1)^* & x_n(m) \end{bmatrix}$$

The null space of a matrix *A* is composed of all vectors *y*, which satisfy

$$\mathrm{Ay} = 0 \tag{7.13}$$

For single user case, there should be more than two antennas at the receiver to ensure the existence of null space. Let Φ_1^T denote the null space of ${H_1}^T$ and Φ_2^T denote the null space of ${H_2}^T$. We have

$$\Phi_1^T \, \widehat{H}_{12}(f_{n,}t) = 0 \tag{7.14}$$

$$\Phi_2^T \, \widehat{H}_{34}(f_{n,}t) = 0 \tag{7.15}$$

$$\widehat{H}\,(f_n, t) = \left[\widehat{H}_{12}(f_{n,}t) \;\; \widehat{H}_{34}(f_{n,}t)\right] \tag{7.16}$$

$$\Phi_1^T \, R_n(m) = \Phi_1^T H(f_{n,}t) X_n(m) + \Phi_1^T n_n(m) \tag{7.17}$$

$$= \left[0 \;\; \Phi_1^T \, \widehat{H}_{34}(f_{n,}t)\right] X_n(m) + \Phi_1^T \, n_n(m)$$

$$\Phi_2^T \, R_n(m) = \Phi_2^T H(f_{n,}t) X_n(m) + \Phi_2^T n_n(m) \tag{7.18}$$

$$= \left[\Phi_2^T \, \widehat{H}_{12}(f_{n,}t) \quad 0\right] X_n(m) + \Phi_2^T \, n_n(m).$$

To simplify the expressions, let us define

$$X_{12} = \begin{bmatrix} x_n(m) & -x_n(m+1)^* \\ x_n(m+1) & x_n(m)^* \end{bmatrix}$$

$$X_{34} = \begin{bmatrix} x_n(m+2) & -x_n(m+3)^* \\ x_n(m+3) & x_n(m+2)^* \end{bmatrix}$$

$$X_n(m) = \begin{bmatrix} X_{12} & -X_{34}^* \\ X_{34} & X_{12}^* \end{bmatrix} \tag{7.19}$$

From the analysis made above, we can see that the QO-STBC with 4 transmit antennas can be decoded in two steps. Each step carries out OSTBC decoding. The symbols are decoded in the second step in a parallel way. With the proposed decoding scheme, the decoding computational complexity can be considerably reduced [20]. We compare the computational loads between the traditional decoding scheme and the one we proposed in terms of times of multiplications and additions needed in the decoding process. As we mentioned above, without loss of generality, we choose the system with a 4 x 4 antennas array. Thus, the coding rate is one. At transmitter, the source bits are mapped to M-QAM constellations [26] to form transmitted symbols. Considering different levels of modulation will cause different computational loads. In this paper, 16-QAM, 64QAM and 256-QAM are considered and their computational loads are calculated separately. We can see that the computational loads are considerably reduced by using our proposed decoding method. With higher bandwidth-efficient modulations, we need longer time to decode QO-STBC signals [35]. With the proposed decoder, the computational complexity with 256-QAM can be reduced to be even lower than that of traditional decoding scheme using I6-QAM. It can be calculated that the decoding complexity can be decreased to roughly 0.3%, taking 256-QAM as an example. To investigate how the decoder will affect the system performance, the symbol error rates (SER) is simulated and compared with the traditional one by choosing the same system parameters. Due to the amplification of the noise power when carrying out the array processing, the SER is thereby degraded a bit. The simulation results is highly coherent with what expected. The SER performance of the proposed decoder is degraded by roughly 3 dB for all the three different QAM constellations. Although there is a bit degradation of the SER performance, the proposed decoder is still of significant utility when the system latency is more important than transmit power. It is worth mentioning that the proposed scheme can also be used in system equipped with more antennas. We also should mention that the existences of the null

spaces are the preconditions which will guarantee the existence of the proposed decoding scheme.

CHAPTER 8

SIMULATION RESULTS

8.1 Simulation Parameters

In this chapter, symbol error rate (SER) performance is investigated for QO-STBC OFDM wireless communication system. Four transmitting and four receiving antennas are used for data transmission. We assume that the channel is time-variant frequency-selective. Channel state information (CSI) is considered to be perfectly known at the receiver and hence, the effects of channel estimation errors do not affect the SER performance.

QO-STBC design uses four time slots and during these four time slots, it is considered that four consecutive OFDM symbols are transmitted. We assume that the channel gain remains constant during these four consecutive OFDM symbols. OFDM technique is used to mitigate the frequency selectivity of multipath fading channel. SER performance is checked for various number of subcarriers. Guard interval (GI) is taken between the adjacent OFDM data blocks, to prevent the inter-carrier interference. Length of GI is taken sufficiently long i.e.

$$N_{GI} T_a \geq \tau_{max}$$

where N_{GI} is the length of guard interval , T_a = sampling time

τ_{max} is the maximum delay spread

Due to sufficient long GI, linear convolution of transmitted data symbols and channel impulses can be expressed as cyclic convolution, which will considerably reduce the computational complexity of the equalizer at the receiver end. In this thesis report, array-processing technique is used to reduce the computational complexity. Array-processing unit at the receiver end, divides the decoding task into two parallel parts. These parallel parts are decoded by the two separate OSTBC decoders, results in reduction of computational complexity at great extent.

Antenna spacing at the transmitter and the receiver is taken sufficient so that there is no spatial correction between the antennas. Fully uncorrelated antennas provide maximum possible diversity gain.

Table 8.1

Parameters used in Computer Simulation

MIMO system parameter	Channel parameters	OFDM system parameters
QO-STBC	Maximum doppler shift f_{max} $\in \{100, 150, 200\}$ Hz	Sampling duration $T_a = 10^{-7}\ s$
Number of transmit antennas $M_{BS} = 4$	$\delta_{BS}/\lambda = 30$	Number of subcarriers $N \in \{64, 128, 256\}$
Number of receiver antennas $M_{BS} = 4$	$\delta_{MS}/\lambda = 3$	Length of Guard interval (GI) $N_{GI} = 21$
Array processing	Total number of path between Base station and mobile unit $\mathcal{L} = 18$	Total duration of one OFDM symbol $T_s = (N + N_{GI})T_\alpha$
Maximum likelihood decoding Modulation techniques used M-QAM, M $\in \{4, 16, 64, \}$	Maximum Doppler Spread $T_{max} = 1050\ ns$	Prefect synchronization and perfect channel state information (CSI)

8.2 Simulation Results

8.2.1 SER Performance for QO-STBC OFDM System using M-QAM

SER performance in QO-STBC wireless communication system is investigated by using different modulation techniques (M-QAM) taking M = 4, 16, 64. The time-variant frequency-selective Rayleigh fading channel is used. Fig. 8.1 shows the variation in SER with respect to the order of modulation scheme. As the order of M-QAM increases, symbol error rate (SER) increases.

With the increase in SNR (dB), gap in SER for different M-QAM is narrow firstly, but after SNR=10 dB(approximately), the gap in SER for different M-QAM modulation

schemes becomes wider. STBC provides diversity gain and allows to use higher order modulation technique.

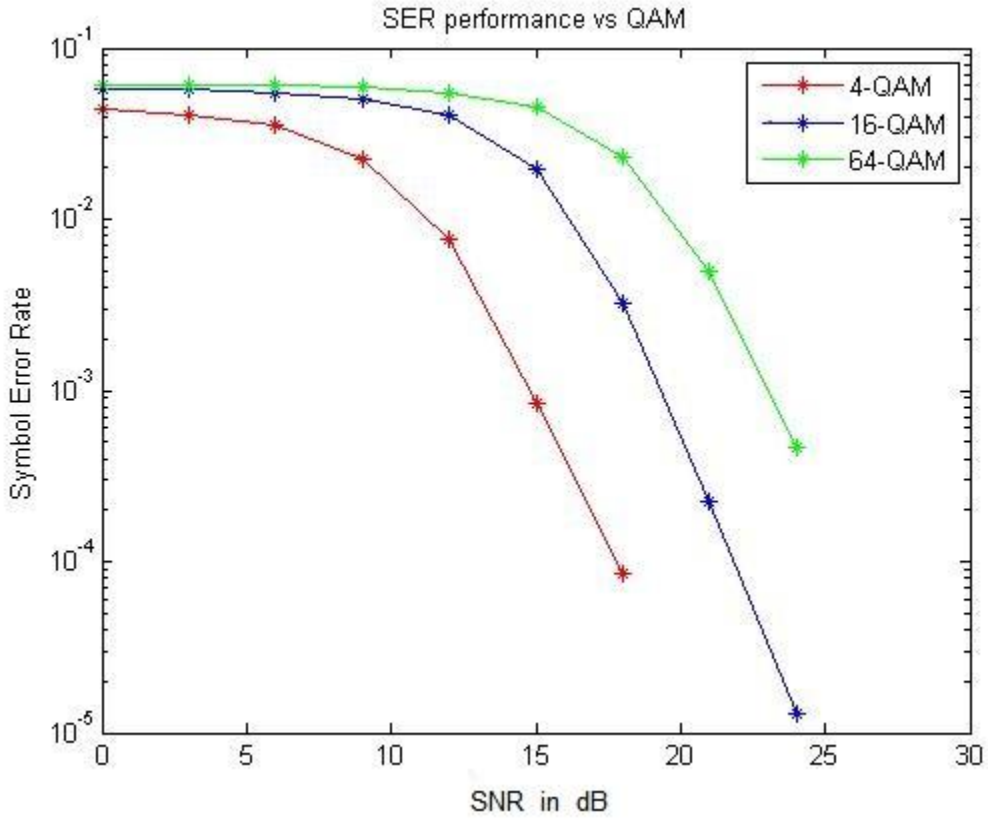

Fig. 8.1 *SER performance for QO-STBC OFDM system in Rayleigh channel using M-QAM.*

In 4-QAM modulation scheme, the value of SER (10^{-3}) is obtained at 15 dB SNR, but in 16-QAM , the same value of SER is obtained at 20 dB (SNR). Transmission rate becomes doubles, but extra 5 dB is required to attain the same SER performance.

8.2.2 SER Performance for QO-STBC OFDM System in Nakagami-m Fading Channel m < 1

SER performance for QO-STBC system is evaluated in Nakagami-m channel for m=0.75. The value parameter m is taken as 0.75. The fading channel is frequency selective. For m=1,

Nakagami channel becomes Rayleigh fading channel. Fig 8.2 shows that the gap between SER for different M-QAM modulation technique increases sharply beyond SNR=5 dB.

Number of subcarrier taken = 64

Order of M-QAM, M = 4, 16, 64.

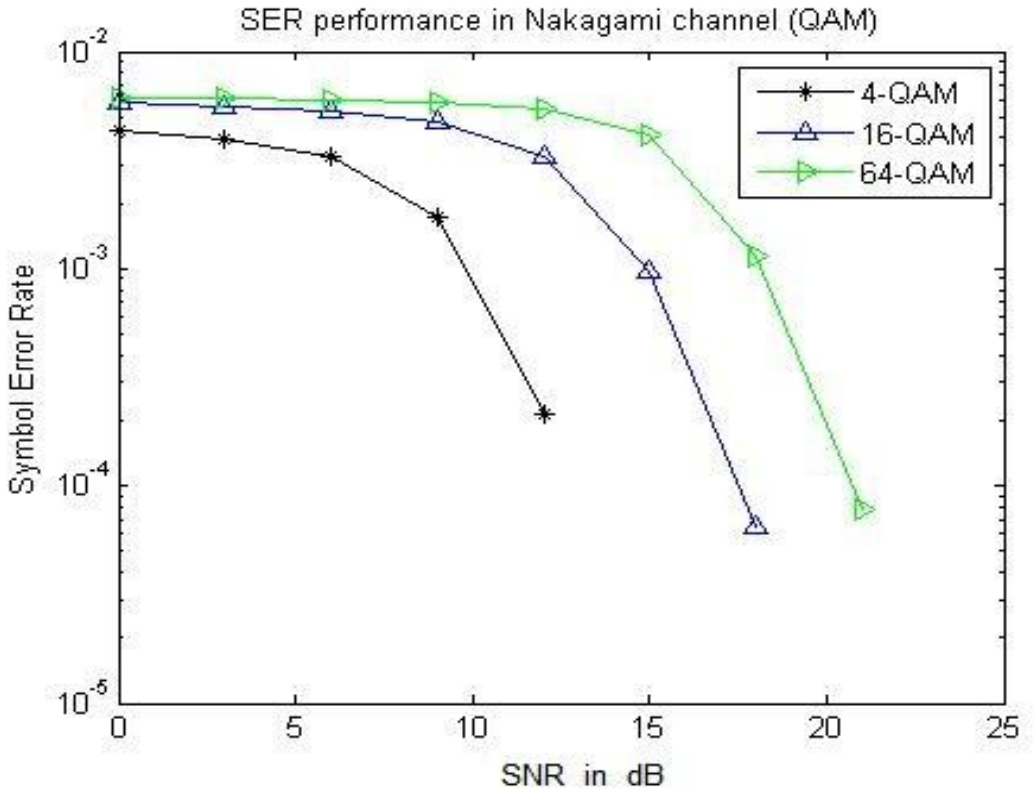

Fig. 8.2 *SER performance for QO-STBC OFDM system in Nakagami-m for m=0.75.*

8.2.3 SER Performance for QO-STBC System in Nakagami-m Fading Channel for m >1 :

SER performance in Nakagami-m fading channel is tested for m = 2 (m >1). The SER decreases with the increase in the value of m. Fig. 8.3 shows the variation in SER with different M-QAM modulation schemes in Nakagami-m fading channel. If we compare the SER performance in Rayleigh and Nakagami-m fading channel, simulation results show that

the SER performance in Nakagami-m fading channel with m=2 is better than the SER performance in Rayleigh fading. The SER (10^{-2}) is obtained in Rayleigh channel at 13 dB (SNR), while SER(10^{-3}) is obtained in case of Nakagami-m fading channel (m=2) at the same value of SNR (13 dB).

To achieve the same SER(10^{-3}) in Rayleigh fading channel, 3 dB extra SNR is required as compared to Nakagam-m fading channel(m=2). Hence, the condition is more favourable in Nakagami-m fading channel with m>1.

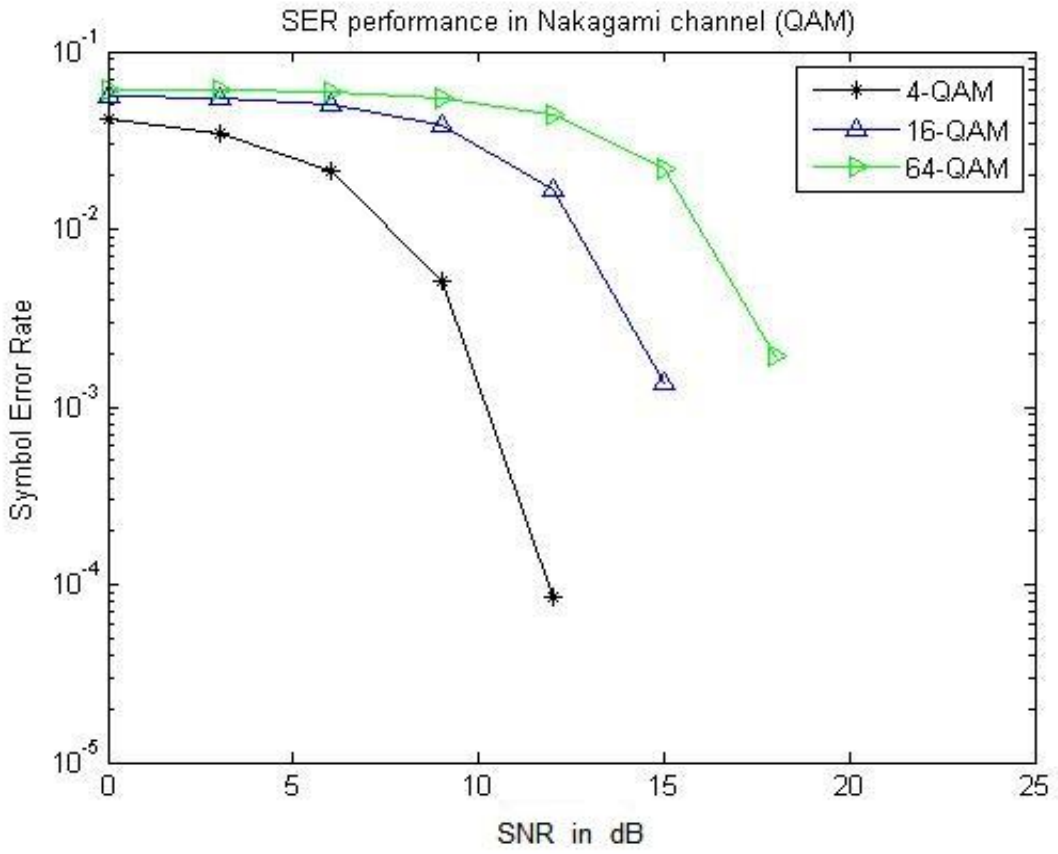

Fig. 8.3 *SER performance for QO-STBC OFDM system in Nakagami-m for m=2.*

8.2.4 SER Performance for QO-STBC System with Different Maximum Doppler Shift

SER performance worsens off when the maximum Doppler shift increases. We assume that the four consecutive OFDM symbols suffer from same fading. It is noted that larger the maximum Doppler shift, larger the mismatch in the frequency response for four consecutive OFDM symbols, which results poor SER performance. For SNR (0-12 dB), SER for different f_{max} = 50, 100, 150 Hz remains almost same, but afterwards, gaps in SER become wider.

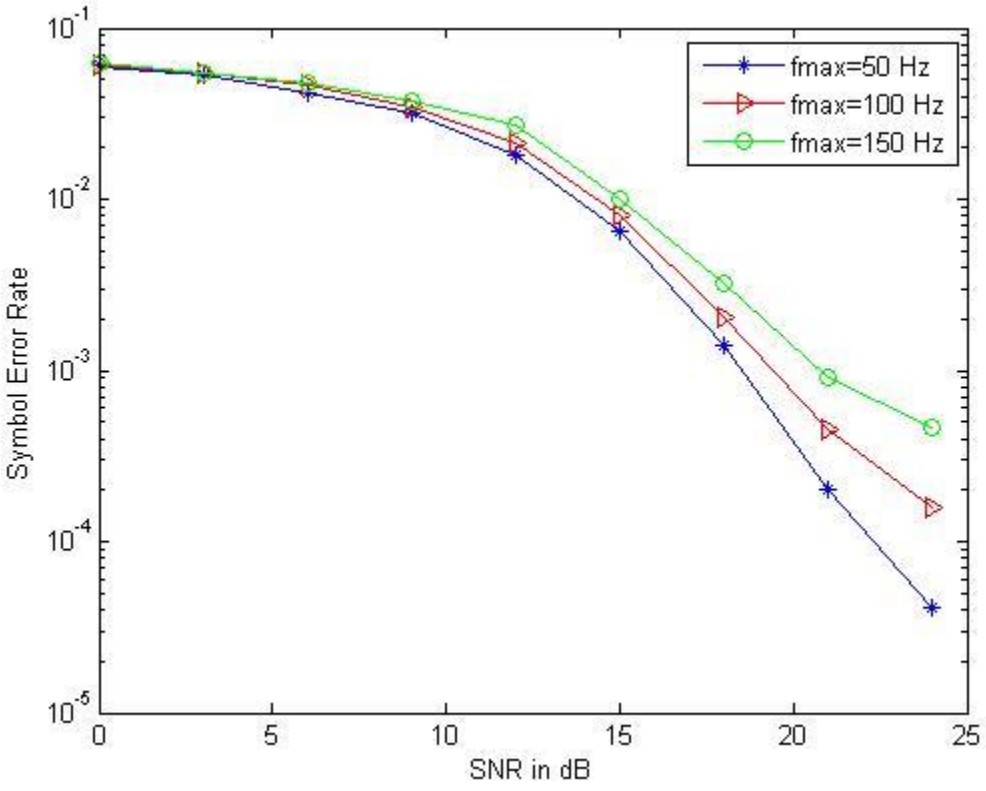

Fig 8.4 *SER performance in QO-STBC OFDM system for different* f_{max} .

8.2.5 SER Performance for QO-STBC System in Rayleigh Fading Channel for Different Number of Subcarriers.

SER performance is getting worse as the number of subcarriers increases. The gap in SER for different FFT size (N = 16, 64, 128) increases reasonably when SNR $\geq$ 7 dB (approximately). As the number of subcarriers increases, inter-carrier interference rises and hence, SER performance decreases. Fig. 8.5 shows that the gap in SER for different number of subcarrier remains almost same as we increase SNR. Larger number of subcarrier indicate large symbol error rate. Due to large number of subcarriers taken, frequency synchronization problems rise.

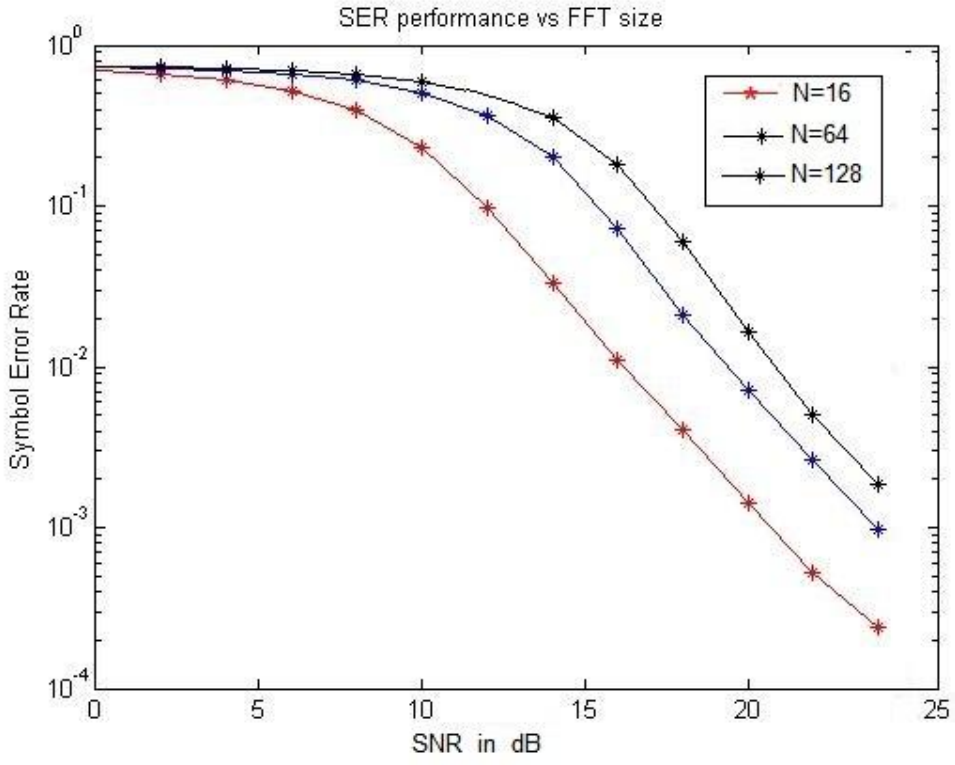

Fig 8.5 *SER performance in QO-STBC OFDM system for different FFT size .*

SER performance degrades with higher level modulation scheme. STBC provides diversity gain, hence allows to use higher level modulation techniques. As the value of parameter m (in Nakagami fading channel) increases, the symbol error rate decreases. For m=1, Nakagami-m channel becomes Rayleigh fading channel. SER performance has also been tested for different maximum Doppler shift. SER performance worsens off when maximum Doppler shift increases, because it is assumed that four consecutive OFDM symbols suffer from same fading. When Doppler shift increases, the mismatch for channel response in four consecutive OFDM symbols becomes larger. SER performance also degrades with the increase in number of subcarriers. Because, as the number of subcarriers increases, the ICI will rise.

Array-processing technique is used in which, received data symbols are converted into parallel streams, each parallel stream is decoded by separate OSTBC decoder. Array Processing technique is very useful in higher level modulation schemes. This technique reduces the computational complexity from M^2 to $2\sqrt{M}$. Array processing based technique reduces complexity with modulation level $2\sqrt{M}$. With the proposed decoder, the computational complexity with 256-QAM can be reduced to be even lower than that of traditional decoding scheme using I6-QAM.

CONCLUDING REMARKS & FUTURE SCOPE

Concluding Remarks

This thesis report presents SER performance analysis in QO-STBC OFDM wireless mobile communication systems. Array-Processing technique is used to reduce computational complexity at the receiver end. Simulation results of SER (symbol error rate) performance in QO-STBC OFDM wireless communication system is evaluated, taking different parameters into account. SER performance is investigated in both Rayleigh and Nakagami-m frequency fading channel for M-QAM modulation technique, M = 4, 16, 64. SER performance degrades with higher level modulation scheme. STBC provides diversity gain, hence allows to use higher level modulation techniques. As the value of parameter m (in Nakagami fading channel) increases, the symbol error rate decreases. For m=1, Nakagami-m channel becomes Rayleigh fading channel. SER performance has also been tested for different maximum Doppler shift. SER performance worsens off when maximum Doppler shift increases, because it is assumed that four consecutive OFDM symbols suffer from same fading. When Doppler shift increases, the mismatch for channel response in four consecutive OFDM symbols becomes larger. SER performance also degrades with the increase in number of subcarriers. Because, as the number of subcarriers increases, the ICI will rise. SER performance in Nakagami-m fading channel with m=2 is better than the SER performance in Rayleigh fading. The SER (10^{-2}) is obtained in Rayleigh channel at 13 dB (SNR), while SER(10^{-3}) is obtained in case of Nakagami-m fading channel (m=2) at the same value of SNR (13 dB).

For decoding of data symbols at the receiver end, Array-Processing technique is used. In this technique, received data symbols are converted into parallel streams, each parallel stream is decoded by separate OSTBC decoder. Array-Processing technique is very useful in higher level modulation schemes. This technique reduces the computational complexity from M^2 to $2\sqrt{M}$. Array processing based technique reduces complexity with modulation level $2\sqrt{M}$. With the proposed decoder, the computational complexity with 256-QAM can be reduced to

be even lower than that of traditional decoding scheme using I6-QAM. It can be calculated that the decoding complexity can be decreased to roughly 0.3 % . Due to the amplification of the noise power when carrying out the array processing, the SER (symbol error rate) performance of the proposed decoder is degraded by roughly 3 dB, which decrease the maximum possible data transmission rate.

Future Scope

In future, SER performance will be investigated by considering the effects of channel estimation errors. Various techniques will be employed to remove the effects of time-varying properties of fading channel.

REFERENCES

[1] S. M. Alamouti, "A simple transmit diversity technique for wireless communications," *IEEE J. Select. Areas Commun.*, vol. 16, pp. 1451-1458, Oct. 1998.

[2] V. Tarokh, H. Jafarkhani and A. R. Calderbank, "Space-time block codes from orthogonal designs," *IEEE Trans. Information Theory*, vol. 45, pp. 1456-1467, Jul. 1999.

[3] Junwoo Jung, Byungchan Kwon and Hyungwon Park, "Superposition-based adaptive modulated space time block coding for MIMO-OFDM systems", *IEEE Communications Letters*, vol. 14, no. 1, pp. 30-32, Jan 2010.

[4] H. Jafarkhani, "A quasi-orthogonal space-time block code," *IEEE Trans. Commun.*, vol. 49, no. 1, pp. 1-4, Jan. 2001.

[5] C. Yuen, Y. Wu and S. Sun, "Comparative study of open-loop transmit diversity schemes for four transmit antennas in coded OFDM systems," *in Proc. IEEE 63th VTC—Fall*, Sep. 2004, pp. 482–485.

[6] W. Su and X. G. Xia, "Signal constellations for quasi-orthogonal space–time block codes with full diversity," *IEEE Trans. Inf. Theory*, vol. 50, no. 10, pp. 2331–2347, Oct. 2004.

[7] C. K. Sung, J. Kim and I. Lee, "Quasi-orthogonal STBC with iterative decoding in bit interleaved coded modulation," in *Proc. IEEE 60th VTC—Fall*, Sep. 2004, pp. 1323–1327.

[8] Minh-Tuan Le, Van-Su Pham, Linh Mai and Giwan Yoon, "Low-complexity maximum-likelihood decoder for four-transmit-antenna quasi-orthogonal space–time block code," *IEEE Trans. Communications*, vol. 53, no. 11, pp. 1817-1821, Nov. 2005.

[9] Erik G. Larsson, Petre Stoica and Jian Li, "On maximum-likelihood detection and decoding for space-time coding systems," *IEEE Trans. Signal Processing*, vol. 50, no. 4, pp. 937-944, April 2002.

[10] S. Chennakeshu and J. B. Anderson, "Error rates for Rayleigh fading multichannel reception of MPSK signals," *IEEE Trans. Commun.*, vol. 43, pp. 338–346, Feb./Mar./Apr. 1995.

[11] Huseyin Arslan, Leonid Krasny, David Koilpillai and Sandeep Chennakeshu , "Doppler spread estimation for wireless mobile radio systems," *IEEE Conference on Wireless Commun. and Networks*, Sept. 2000, pp. 1075-1079.

[12] Trym H. Eggen, James C. Preisig, and Arthur B. Baggeroer, "Communication over doppler spread channels—ii : Receiver characterization and practical results," *IEEE Journal of Oceanic Engineering*, vol. 26, no. 4, pp. 612-621, Oct. 2001.

[13] Lu Qiaoli, Chen Wei,Xie Tao, and Long Biqi, "A doppler spread estimator design for mobile OFDM systems," *IEEE Conference on Commun. Systems*, Mar. 2008, pp. 1046-1050.

[14] Kuo-Hui Li and Mary Ann Ingram, "Space–time block-coded OFDM systems with RF beamformers for high-speed indoor wireless communications," *IEEE Transactions on Communications*, vol. 50, no. 12, pp. 1899-1901, Dec. 2002.

[15] Jaeho Chug, Jaehwa Kim, Taekon Kim and Jaemoon Jo, "Performance evaluation of MIMO-OFDM systems in correlated fading channels," *CCECE, Niagara Falls*, May 2004, pp. 457-460.

[16] Enis Akay and Ender Ayanoglu, "Bit interleaved coded modulation with space time block codes for OFDM systems," *IEEE Conference*, May 2004, pp. 2477-2481.

[17] Zhuo Chen, Zhanjiang Chi, Yonghui Li, Branka Vucetic and Hajime Suzuki, "Analysis of maximal-ratio combining with transmit antenna selection in flat Nakagami-m fading channels for arbitrary m*," IEEE Conference*, 2007 , pp. 1102-1107.

[18] J. W. Craig, "A new, simple and exact result for calculating the probability of error for two-dimensional signal constellations," in *Proc. IEEE Military Communications Conf. MILCOM'91* McLean, VA, Oct. 1991, pp. 571–575.

[19] Tzi-Dar, Tsai, *OFDM baseband receiver design for wireless communication*, John Wiley & Sons pvt. ltd.

[20] Haixia Zhang, Dongfeng Yuan and Hsiao-Hwa Chen, **"**Array-processing-based quasi-orthogonal space–time block-coded OFDM systems", *IEEE Trans. on Vehicular Technology*, vol. 59, no. 1, pp. 508-513, Jan 2010.

[21] Schmidl, T. M. and D. C. Cox, ''Robust frequency and timing synchronization for OFDM,'' *IEEE Trans. Comm.*, vol. 45, pp. 1613–1621, April 1996.

[22] P. H. Moose, ''A technique for OFDM frequency offset correction,'' *IEEE Trans. Comm.*, vol. 42, no. 10, pp. 2908–2914, Oct. 1994.

[23] B. Vucetic and J. Yuan, *Space-Time Coding*, Chichester, UK, John Wiley & Sons ltd., 2003.

[24] G. B. Giannakis, Z. Liu, X. Ma and S. Zhou, *Space-time coding for broadband wireless communications*. Wiley, 2007.

[25] L. Azzam and E. Ayanoglu, "Reduced complexity sphere decoding for square QAM via a new lattice representation," *in Proc. IEEE Global Telecommun. Conf.*, Nov. 2007, pp. 4242-4246.

[26] X. Li, T. Luo, G. Yue and C. Yin, "A squaring method to simplify the decoding of orthogonal space-time block codes," *IEEE Trans. Commun.*, vol. 49, pp. 1700-1703, Oct. 2001.

[27] J. Kim and I. Lee, "Space–time coded OFDM systems with four transmit antennas*," in Proc. IEEE 60th VTC—Fall, Sep. 2004*, vol. 2, pp. 2434–2438.

[28] C. Yuen, Y. L. Guan and T. T. Tjhung, "Quasi-orthogonal STBC with minimum decoding complexity," *IEEE Trans. Wireless Commun.*, vol. 4, no. 5, pp. 2089–2094, Sep. 2005.

[29] M. Le, V. Pham, L. Mai and G. Yoon, "Low-complexity maximum likelihood decoder for four-transmit-antenna quasi-orthogonal space–time block code," *IEEE Trans. Commun.*, vol. 53, no. 11, pp. 1817–1821, Nov. 2005.

[30] L. He and H. Ge, "Fast maximum likelihood decoding of quasi-orthogonal codes*," in Proc. Asilomar Conf. Signals, Syst., Comput.*, Nov. 2003, vol. 1, pp. 1022–1026.

[31] C. Jiang, H. Zhang, D. Yuan, and H. H. Chen, "A low complexity decoding scheme for quasi-orthogonal space–time block coding," *in Proc. 5th IEEE Sens. Array Multi-Channel Signal Process.* Workshop, 2008, pp. 9-12.

[32] M. Paetzold and B. Õ. Hogstad, "A wideband space–time MIMO channel simulator based on the geometrical one-ring model*," in Proc. 64th IEEE Semi-Annu. VTC—Fall*, Sep. 2006, pp. 1–6

[33] B. Sklar, "Rayleigh Fading Channels in Mobile Digital Communication Systems- Part I: Characterization*," IEEE Commun. Mag.*, vol 35, pp. 90-100, July 1997.

[34] S. Sandhu and A. Paulraj, "Space–time block codes: A capacity perspective," *IEEE Commun. Lett.*, vol. 4, pp. 384–386, Dec. 2000.

[35] N. Sharma and C. B. Papadias, "Improved quasi-orthogonal codes through constellation rotation," *IEEE Trans. Commun.*, vol. 51, pp. 332-335, Mar. 2003.

[36] C. B. Papadias and G. 1. Foschini, "A space-time coding approach for systems employing four transmit antennas," *Proc. IEEE ICASSP'OI, Salt Lake City, USA, 2001*, vol. 4, pp. 2481-2484.

[37] W. C. Jakes, Ed., *Microwave Mobile Communications*, New York: Wiley, 1974.

[38] G. H. Golub and C. F. Van Loan, *Matrix Computations*, 3rd ed. Baltimore, MD: Johns Hopkins Univ. Press, 1996.

[39] O. Damen, A. Chkeif and J. C. Belfiore, "Lattice code decoder for space–time codes," *IEEE Commun. Lett.*, vol. 4, no. 5, pp. 161–163, May 2000.

[40] M. Le, V. Pham, L. Mai and G. Yoon, "Low-complexity maximum likelihood decoder for four-transmit-antenna quasi-orthogonal space-time block code," *IEEE Trans. Commun*., vol. 53, no. 11, pp. 1817-1821, Nov. 2005.

[41] B. M. Hochwald and S. ten Brink, "Achieving near-capacity on a multiple- antenna channel," *IEEE Trans. Commun.*, vol 24, pp. 467-473, May 2001.

[42] Classen, F., and H. Meyr, ''Frequency synchronization algorithms for OFDM systems suitable for communication over frequency-selective fading channels,'' *IEEE Vehic. Technol. Conf.*, vol. 3, Stockholm, Sweden, June 1994, pp. 1655–1659.

[43] Daffara, F. and A. Chouly, ''Maximum likelihood frequency detectors for orthogonal multicarrier systems,'' *Proc. Intern. Conf. Commun.*, Switzerland, May 1993, pp. 766–771.

[44] Proakis, J., *Digital Communications*, New York: Prentice-Hall, 3rd edition, 1995.

[45] Jankiraman, M. and R. Prasad, ''A novel algorithmic synchronization technique for OFDM-based wireless multimedia communications,'' *ICC '99 Proceedings,* Vancouver, Canada, 2004, pp. 271-275.

[46] A. Glavieux, P. Y. Cochet and A. Picart, "Orthogonal frequency division multiplexing with BFSK modulation in frequency selective Rayleigh and Rician fading channels," *IEEE Trans. Commun.*, vol. 42, no. 2–4, pp. 1919–1928, Feb./Mar./Apr. 1994.

[47] J. Lu, T. T. Tjhung, F. Adachi, and C. L. Huang, "BER performance of OFDM-MDPSK system in frequency-selective Rician fading with diversity reception," *IEEE Trans. Veh. Technol.*, vol. 49, no. 7, pp. 1216–1225, Jul. 2000.

[48] M. Nakagami, "The m-distribution, a general formula of intensity distribution of rapid fading," in *Statistical Methods in Radio Wave Propagation*, W. G. Hoffman, Ed. Oxford, U.K.: Pergamon, vol 36, pp. 478-484, March 1960.

[49] T. Eng and L. B. Milstein, "Coherent DS-CDMA performance in Nakagami multipath fading," *IEEE Trans. Commun.*, vol. 43, no. 2–4, pp. 1134–1143, Feb./Mar./Apr. 1995.

[50] M. S. Alouini and A. J. Goldsmith, "A unified approach for calculating error rates of linearly modulated signals over generalized fading channels," *IEEE Trans. Commun.*, vol. 47, no. 9, pp. 1324–1334, Sep. 1998.

[51] L.-L. Yang and L. Hanzo, "Performance of generalized multicarrier DS-CDMA over Nakagami-mfading channels," *IEEE Trans. Commun.*, vol. 50, no. 6, pp. 956–966, Jun. 2002.

[52] A. Scaglione, S. Barbarossa, and G. B. Giannakis, "Optimal adaptive precoding for frequency-selective Nakagami-m fading channels," in *Proc. 52nd IEEE Veh. Technol. Conf.*, vol. 3, June 2000, pp. 1291–1295.

[53] A. Papoulis, *Probability, Random Variables, and Stochastic Processes*, 3rd edition, New York: McGraw-Hill, 1991.